J Comput Neurosci (2006) 21:51–70
DOI 10.1007/s10827-006-7199-6

A model that integrates eye velocity commands to keep track of smooth eye displacements

Gunnar Blohm · Lance M. Optican · Philippe Lefèvre

Received: 31 August 2005 / Revised: 12 January 2006 / Accepted: 13 January 2006 / Published online: 22 April 2006

Abstract Past results have reported conflicting findings on the oculomotor system's ability to keep track of smooth eye movements in darkness. Whereas some results indicate that saccades cannot compensate for smooth eye displacements, others report that memory-guided saccades during smooth pursuit are spatially correct. Recently, it was shown that the amount of time before the saccade made a difference: short-latency saccades were retinotopically coded, whereas long-latency saccades were spatially coded. Here, we propose a model of the saccadic system that can explain the available experimental data. The novel part of this model consists of a delayed integration of efferent smooth eye velocity commands. Two alternative physiologically realistic neural mechanisms for this integration stage are proposed. Model simulations accurately reproduced prior findings. Thus, this model reconciles the earlier contradictory reports from the literature about compensation for smooth eye movements before saccades because it involves a slow integration process.

Action Editor: Jonathan D. Victor

G. Blohm · P. Lefèvre
CESAME, Université catholique de Louvain,
4, avenue G. Lemaître 1348 Louvain-la-Neuve, Belgium;
Laboratory of Neurophysiology, Université catholique de
Louvain, 1200 Brussels, Belgium
e-mail: lefevre@csam.ucl.ac.be

G. Blohm (✉)
Centre for Vision Research, York University,
Toronto Ontario M3J 1P3, Canada
e-mail: blohm@yorku.ca

L. M. Optican · P. Lefèvre
Laboratory of Sensorimotor Research, National Eye Institute,
NIH, Bethesda, MD 20892

Keywords Saccades · Smooth pursuit · Updating · Double step · Remapping

Introduction

The oculomotor system uses different control modes to orient the visual axis in space. Fast eye movements (saccades) reposition the line of sight, whereas smooth pursuit movements track slowly moving stimuli. In natural viewing conditions, the smooth pursuit and saccadic motor systems work synergistically to optimize vision. This synergy is supported by the overlap of neuronal circuits underlying both types of eye movement (for reviews, see Krauzlis and Stone, 1999; Krauzlis, 2004). One of the major inputs shared by both the saccadic and smooth pursuit systems is target velocity (Newsome et al., 1985; Keller and Johnsen, 1990; Gellman and Carl, 1991; Smeets and Bekkering 2000; de Brouwer et al., 2001; de Brouwer et al., 2002a; de Brouwer et al., 2002b). The saccadic system needs a position input to correct retinal displacement errors, but it also uses a retinal velocity signal to compute the trigger time and amplitude of saccades to moving visual targets. However, in the absence of visual information about eye and target motion, the system cannot rely on those signals and must use other mechanisms to execute spatially accurate saccades.

Almost two decades ago, McKenzie and Lisberger (1986) performed an experiment that was designed to test whether saccades were directed to an absolute eye position in space or were determined by a desired eye displacement. They argued that if actual eye position was compared to a desired spatial position, saccades to memorized targets should always be accurate, even when the eyes move smoothly during the period between the target presentation and the resulting

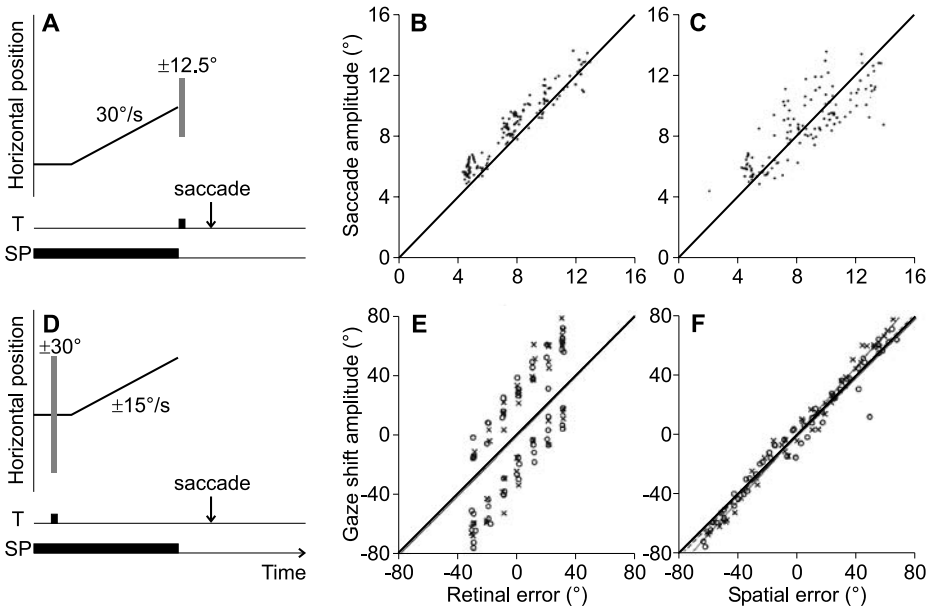

Fig. 1 Contradictory data from literature. (A). Experimental paradigm from McKenzie and Lisberger (1986). The target (T) was flashed for 10 ms at the moment of the smooth pursuit target (SP) disappearance. Monkeys had to orient their gaze towards the flash (T) as soon as they could. (B, C). Results adapted from McKenzie and Lisberger (1986) for the programming of saccades to targets flashed at the moment of extinction of a pursuit target. The saccades were initiated with latencies around 180 ms after the flash (T) presentation. The amplitude of these saccades was predicted by the retinal error (panel B) and saccades were thus spatially inaccurate (panel C). (D). Experimental paradigm from Herter and Guitton (1998). The target (T) was flashed for 50 ms before the onset of the smooth pursuit (SP) movement. Human subjects were instructed to make a gaze movement towards the remembered flash (T) location after the disappearance of the smooth pursuit target (SP). The smooth pursuit target duration varied between 1 s and 2 s. This resulted in very long latencies (latencies measured with respect to the flash presentation). (E, F). Results adapted from Herter and Guitton (1998) concerning the accuracy of saccades to targets flashed before smooth pursuit. Panel F shows that the amplitude of head-free open circle as well as head-fixed (cross) gaze saccades followed the spatial error. The retinal error hypothesis did not predict their amplitude (panel E). Solid lines in panels B, C, E and F show the theoretically optimal retinal or spatial saccade behavior

saccade. Using such a "smooth double-step[1]" paradigm (Fig. 1(A)), they reported that this prediction was incorrect (McKenzie and Lisberger, 1986); their monkeys systematically made inaccurate eye movements that were appropriate for the target's retinal error. Fig. 1(B) and (C) summarize these findings. The scatter of the data around the optimal behavior represented by the solid line shows a better correlation of saccade amplitude with the retinal (Fig. 1(B)) as opposed to the spatial (Fig. 1(C)) error hypothesis. These results were confirmed by Gellman and Fletcher (1992) for smooth pursuit and by Blohm et al. (2003, 2005) for short latency saccades during smooth anticipatory eye movements and during smooth pursuit, respectively. Of course, this lack of spatial accuracy is only present if the saccadic system cannot use retinal velocity information for a predictive adjustment of the motor command, e.g., when the target is presented very briefly (less than $\sim$50 ms).

In contrast with these rapidly programmed retinotopic saccades, several studies reported that saccades aimed at the location of targets memorized before or during smooth pursuit were spatially accurate (Schlag et al., 1990; Ohtsuka, 1994; Zivotofsky et al., 1996; Herter and Guitton, 1998; Baker et al., 2003). This is illustrated in Fig. 1(E) and (F), where we reproduce the findings of Herter and Guitton (1998). In these studies subjects were instructed to make a memory-guided saccade only after the end of the smooth pursuit movement (as compared to the reactive short-latency saccades in the above-described investigations). Clearly, saccades here are better correlated with the spatial error hypothesis (Fig. 1(F)) than with the retinal error hypothesis (Fig. 1(E)). The major difference between saccades in these studies and those reporting retinotopically programmed saccades was the latency of saccade execution with respect to target appearance. Whereas retinotopically programmed saccades were naturally triggered by the presentation of the target (mean latencies $<$300 ms), spatially accurate saccades occurred after an additional delay period between the presentation of the memorized target and the orienting saccade

[1] The "smooth double-step" paradigm was conceived as an analog of the classical "double-step" paradigm, where two targets are presented in rapid succession before the saccade towards the first target. Then, the movement vector from the first to the second target is different from the retinal information and extraretinal signals about the first saccade needs to be taken into account to update the second saccade vector. In the "smooth double-step" paradigm, the first saccadic step is replaced by a smooth pursuit eye movement, therefore the name.

(mean latencies >600 ms). This difference in latencies suggests that a retinal-to-spatial transformation for the internal coding of memorized targets can only occur if enough time is available.

The hypothesis of a transformation that takes time to change from a retinotopic to a spatial encoding has been addressed in two recent studies of smooth pursuit (Blohm et al., 2005) and smooth anticipatory eye movements (Blohm et al., 2003). In these studies, the "smooth double-step" paradigm was used. The authors analyzed the first orienting eye movements, as in previous studies, and also analyzed secondary saccades. As a result, Blohm et al. (2003, 2005) obtained a much wider range of saccade latencies than previous studies and were thus able to demonstrate that extraretinal information about smooth eye displacement was delayed ($\sim$ 175 ms) with respect to the smooth eye movement. Consequently, longer latency saccades (>175 ms) used the *available* smooth eye displacement information to compensate for smooth eye motion. These results reconcile previous contradictory findings of uncompensated, retinotopic, coding (McKenzie and Lisberger, 1986; Gellman and Fletcher, 1992) and compensated, spatially accurate saccades (Schlag et al., 1990; Ohtsuka, 1994; Zivotofsky et al., 1996; Herter and Guitton, 1998; Baker et al., 2003).

It is worth mentioning that this delayed retinal-to-spatial transformation of smooth eye displacement is specific to smooth movements, and has not been observed for the saccadic system, i.e. there is no delay between a saccadic eye movement towards a target and the internal spatial updating of the target position. Indeed, the use of extraretinal signals to maintain space constancy has been extensively studied by means of the so-called "double-step" and "colliding saccades" paradigms (Hallett and Lightstone, 1976a, b; Becker and Jürgens, 1979; Mays and Sparks, 1980; Aslin and Shea, 1987; Schlag et al., 1989; Schlag and Schlag-Rey, 1990; Dassonville et al., 1992; Dominey et al., 1997; Goossens and Van Opstal, 1997; Mushiake et al., 1999; Tian et al., 2000). In these experimental conditions, a saccadic eye movement was evoked either visually (double-step) or by microstimulation (colliding saccades) during the latency period before a saccade to a previously memorized target. Despite this perturbation, orienting saccades remained spatially accurate even for very short intervals between two consecutive saccadic eye movements. The authors concluded that the saccadic system has access to extraretinal signals about previous saccadic eye movements to update the internal target representation in space. This allows the visual system to ensure space constancy, i.e. an accurate spatial perception of the world despite retinal shifts due to self-motion.

Current saccadic models cannot explain the delayed retinal-to-spatial transformation reported for saccades to targets memorized before a smooth eye displacement. Here, we propose a new model of the saccadic system that can account for the "smooth double-step" data available today. We developed two different hypothetical, physiologically realistic neural mechanisms which compute a delayed internal estimate of the smooth eye displacement. The smooth eye velocity integration mechanisms fit both our data and previous observations in the literature. Since behavioral experiments cannot distinguish between those two hypotheses, we suggest a series of electrophysiological experiments to identify the correct mechanism.

Methods

First, we will provide a general overview of the saccadic model we developed to account for the "smooth double-step" results. The crucial original contribution of this model was a smooth eye velocity integration stage that was necessary to estimate the smooth eye displacement (SED). In the second and third part of this section, we will describe two physiologically realistic neural mechanisms that could perform this velocity-to-position transformation step and provide an SED estimate to the target memory structure of the brain. Finally, we will briefly introduce an experimental data set that was used to fit the model simulation parameters, and describe how we reproduced data from the literature.

The saccadic pathway

Figure 2 shows the basic structure of the saccadic model we developed. We used retinal position error (PE_R = constant) and time varying eye velocity (EV) as inputs to the model. The position memory structure had two internal target representations in retinal and spatial coordinates. The input PE_R was memorized (Fig. 2: position memory) to represent the target position in retinal coordinates. The spatial representation of the same target was updated by the amplitude (S_{AMP}) of executed saccades (more than one saccade could occur). This was done to implement the remapping (also called updating) of the internal representation of memorized targets after saccades (Henriques et al., 1998; Medendorp et al., 2002; Merriam et al., 2003). In addition to spatial updating by saccades, the eye velocity (EV) integration mechanism (Fig. 2: EV integration) also provided an instantaneous estimate of the smooth eye displacement (SED_{est}) to update the spatial stimulus representation in the position memory structure. Therefore, once a saccade was triggered, the saccade generator (Fig. 2) used the latest available remaining error ΔE (before the saccade was triggered) of the spatial target representation (in retinotopic coordinates) to build the saccadic drive. Here, we did not model the saccade trigger mechanism but used instead the time of saccade occurrence from experimental data (see Discussion section). To complete the model, the smooth and saccadic eye movement

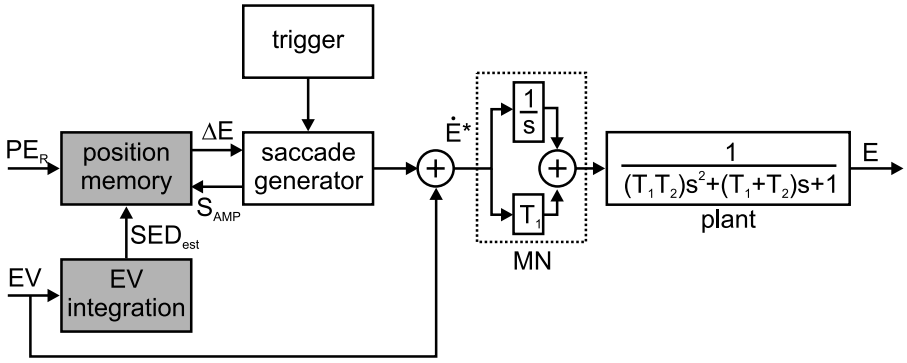

Fig. 2 General model structure. The inputs were retinal position error (PE_R) and eye velocity (EV) over time. An eye velocity integration mechanism provided an instantaneous estimation of the smooth eye displacement (SED_{est}) to a target position memory structure. There was thus a velocity-to-position transformation of EV. The internal representation of target position (memory) was updated by SED_{est} and the actual saccade amplitude (S_{AMP}) each time a saccade occurred. Once a saccade was triggered, the saccade generator produced a motor command that was added to the smooth eye velocity. This approximation of the desired eye velocity $\dot{E}^*$ is sent in parallel to a direct and an integral pathways (motor neurons: MN) that compensate for the eye plant dynamics and provide the pulse-step motor command which in turn is sent through the eye plant low-pass filter to provide eye position (E). The grey boxes indicate the novel parts of the model

commands were added before sending the final motor command to the motor neurons and the eye plant (Fig. 2: MN and plant).

For the saccade generator (Fig. 2), we used a classical structure (modified from Jürgens et al., 1981). The position error ΔE was sent through a gain element (gain = 0.9 to account for the saccadic undershoot strategy). This provided the desired eye movement that was compared to the executed eye movement to produce the motor error. This motor error was sent to a pulse generator, the output of which was the saccadic motor command $\dot{E}^*$ sent to the motor neurons (MN) and eye plant (Fig. 2: MN and plant). For the pulse generator, we used the following "bi-lateral" version of the burst neurons discharge rate proposed by van Gisbergen et al. (1981):

$$y = \begin{cases} -b_m \cdot \left(1 - \exp^{\frac{x-e_0}{b_k}}\right) & \text{if } x < -e_0 \\ b_m \cdot \left(\exp^{\frac{x-e_0}{b_k}} - \exp^{\frac{-x-e_0}{b_k}}\right) & \text{if } -e_0 \le x \le e_0 \\ b_m \cdot \left(1 - \exp^{\frac{-x-e_0}{b_k}}\right) & \text{if } x > e_0 \end{cases} \quad (1)$$

The input x was the motor error and the output y was an approximation of the saccadic velocity command. We used parameters close to the ones used by van Gisbergen et al. (1981), i.e. $e_0 = 1\,\text{deg}$, $b_m = 600\,\text{deg/s}$ and $b_k = 3\,\text{deg}$. The function in Eq. (1) provides a good fit of the experimental data. The final pulse-step generation pathway of the motor neurons (MN) consisted of the sum of the motor command (multiplied by $T_1 = 175$ ms) and its integral (Robinson, 1970). The eye plant (Fig. 2: plant) was modeled by a second order system with time constants $T_1 = 175$ ms and $T_2 = 13$ ms (Robinson, 1973) acting as a low-pass filter. It should be mentioned that the purpose of this saccadic model implementation was not to reproduce exactly the saccade dynamics but only to embed the smooth eye velocity integration mechanism in a global framework. Next, we will describe the two hypotheses for estimating smooth eye displacement, i.e. the place-code and rate-code mechanisms.

Rate code displacement estimation mechanism

The rate code smooth eye displacement estimator used two computational stages. The first stage was composed of a series of neural cells with different tuning curves (TC) for the eye velocity (EV) input (Fig. 3(A)). Therefore, the output (a_{VSC}) of these velocity sensor cells (Fig. 3(A): VSC) depended on EV through a normalized log-normal function.

$$a_{VSC}(EV) = \left\langle \frac{1}{EV \cdot \sigma\sqrt{2\pi}} \cdot \exp\left(\frac{-(\ln(EV) - \mu)}{2\sigma^2}\right)\right\rangle \quad (2)$$

where $\mu = \ln(m) + \sigma^2$, m was the maximum of the log-normal function (= preferred velocity of the cell) and $\sigma = m^{-4}$ was its standard deviation. The triangular brackets indicate the normalization of the function with respect to the maximum, i.e. $a_{VSC}(m) = 1$. The shape of this function is represented in Fig. 3(B). We chose this log-normal expression of the tuning curve (TC) characteristics because this appeared to be a physiologically realistic form (Maunsell and Van Essen, 1983; Felleman and Kaas, 1984; Cheng et al., 1994; DeAngelis and Uka, 2003). However, the exact shape of the velocity sensor cell's input-output relationship was not important and did not fundamentally affect the results.

For the simulations presented here, we used $N = 20$ velocity sensitive cells characterized by preferred velocities with squared distances $m_i = \left[0.5^2, 1, 1.5^2, 2^2, \ldots, 10^2\right]$. This particular choice accounted for the increasing width of TC with increasing m_i, to ensure approximately constant overlap of the TC shapes (Maunsell and Van Essen, 1983).

The second, main stage of the rate code mechanism integrated the velocity sensor cell's output (see Fig. 3A: INT). Each velocity sensor neuron projected to one and only one integration neuron. This integration stage was implemented as follows:

$$T_N \frac{da_{\mathrm{INT}}}{dt} = k \cdot a_{\mathrm{VSC}} \tag{3}$$

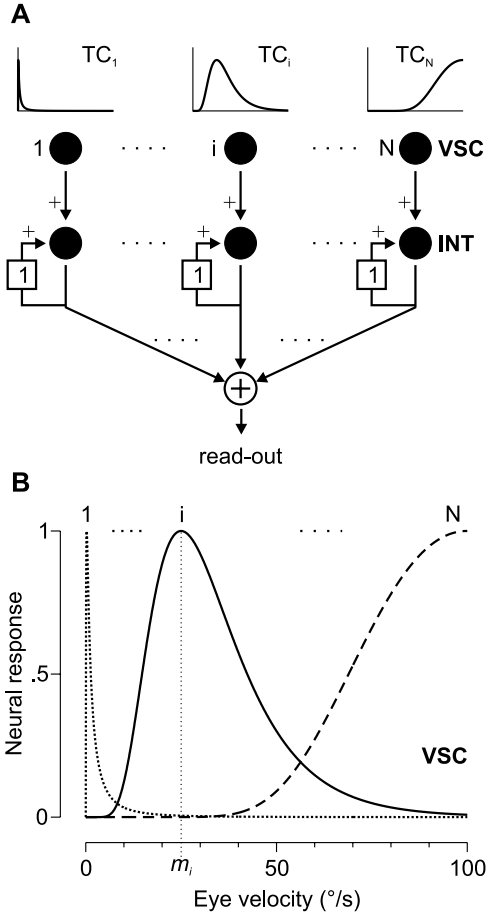

Fig. 3 Rate code mechanism. (A). Model structure. Two layers of neurons were used. The first layer consisted of eye velocity sensitive cells (VSC) with log-normal tuning curves (TC). The output of these velocity sensor cells was normalized with respect to the distribution's maximum (see Eq. (2)). The second layer (INT) integrated the output of the first layer (Eq. (3)) using a perfect integrator (feedback gain = 1). The read-out of this group of INT cells was performed by summing their output weighted by the preferred velocity of each column (Eq. (4) and (5)). B. Shape of tuning curves (Eq. (2)) for VSC cells. Three examples of tuning curves for cells with different preferred velocities m_i are shown (dotted: 0.25°/s; solid: 25°/s; dashed: 100°/s)

T_N was a constant gain representing the natural time constant of the cells (we used $T_N = 3$ ms) and k was an accumulation gain that took into account the simulation time step, i.e. $k = 1/dT$, where $dT = 1$ ms was the simulation time step. INT cells thus integrated the output of VSC cells weighted by the gain k to account for the size of the simulation time step dT. The level of activity of an integration cell $a_{\mathrm{INT},i}$ was therefore an approximation of the time during which the eye velocity was close to m_i. To illustrate this, consider one preferred velocity column and imagine that the eye velocity corresponds to preferred velocity m_i of this column. Then, the output of VSC cells is 1. INT cells thus receive in each time step the input 1 to integrate. Since we performed the simulations in millisecond timescale, the output of the INT cell will indicate the time during which the VSC cell was fully activated.

The readout of these integrator cells was calculated as a weighted sum $WS(t)$ of the integration cell's activities. This read-out provided an estimate of the smooth eye displacement $SED_{\mathrm{est}}(t)$ in the following way (Fig. 3A: read-out):

$$T_{RO} \cdot \frac{dSED_{\mathrm{est}}(t)}{dt} = -SED_{\mathrm{est}}(t) + c \cdot WS(t) \tag{4}$$

$$WS(t) = \sum_{i=1}^{N} m_i \cdot a_{\mathrm{INT},i}(t) \tag{5}$$

T_{RO} was the time constant of the read-out neuron's activity and was adjusted to produce the observed delay (Blohm et al., 2003, 2005) between the smooth eye movement and its compensation. This is equivalent to a high-gain, low-pass filter of the neural activity read-out. The constant c was adapted to match $SED_{\mathrm{est}}(t)$ with the real smooth eye displacement and accounted for the different subjects' individual overall compensation gain. Note that this model did not assume any topographically arranged neurons, since they did not interact with their neighbors. (We chose to integrate the output of each VSC neuron before the weighted summation process, instead of integrating the weighted summation of the all the VSC cells; both are equivalent in this linear system.) This architecture is inherently stable and has only two free parameters, i.e., the read-out time constant T_{RO} and the gain c.

Place code mechanism

The place code mechanism represented smooth eye displacement on a topographical position map. The only input to this displacement map was eye velocity (EV). The mechanism assumed that the flash's appearance initialized the system by resetting the displacement map. This was done by activating

the neurons of the map at the site corresponding to zero displacement (we used a unit-height Gaussian pulse with $\mu = 0^\circ$ and $\sigma = 1^\circ$ to represent the initial distribution of activity). Afterwards, a neural mechanism (described below) made the activity spread as a function of eye velocity. The read-out of the map provided the instantaneous estimate of smooth eye displacement. Figure 4A shows the basic structure of this mechanism.

We used a row of 51 topographically arranged neurons, where neuron #26 corresponded to zero displacement.

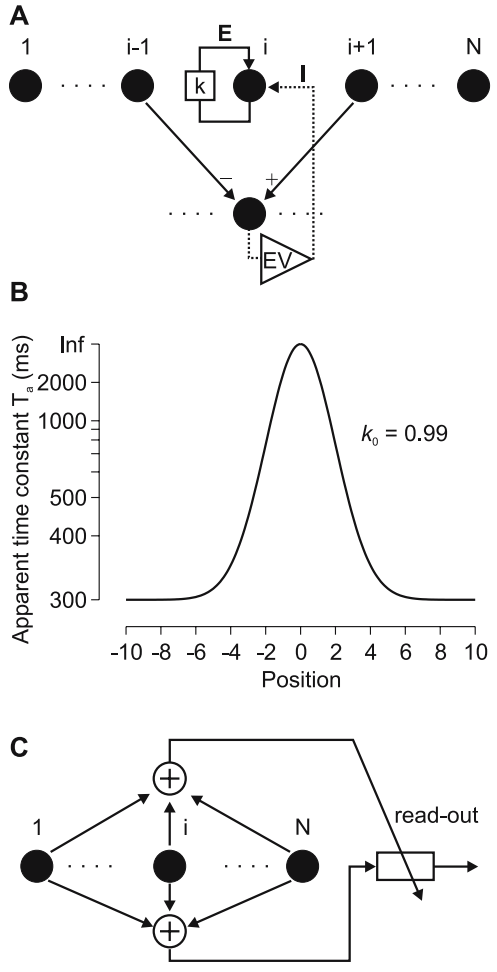

Fig. 4 Place code mechanism. (A). Structure of the displacement map. Neuron i has input from itself (E, reverberation constant k) and from the neighboring neurons (I). The reverberation gain depends on the location of the maximum activity on the map (Eq. (10)). The input I from the neighbors is an eye velocity weighted signal representing the strictly positive part of the map's activity gradient (Eq. (7), (8) and (9)). (B). The apparent time constant T_a of the map activity is presented on a reciprocal scale over position for $k_0 = 0.99$. The position is relative to the location of the maximum activity on the displacement map. C. The read-out procedure of the map consists of computing the center of activity (COA). The sum of the map's neurons weighted output (weighted by the neuron's position x_i) is scaled by the total map activity (Eq. (12))

The basic dynamics of the map's neural activity, a_{map}, was described by the following rate equation:

$$T_N \cdot \frac{da_{\text{map}}}{dt} = -a_{\text{map}} + I + E \tag{6}$$

$T_N = 3$ ms was the neural time constant. I described the input from the neighboring neurons and E was the self-excitation (see Fig. 4A). The input I of the neighboring neurons to a neuron i (Fig. 4A) was calculated by taking the positive results (as neurons do not fire negatively) of the difference between the two neighboring neurons' activity, weighted by eye velocity. The eye velocity thus modulates the synaptic weights of the activity difference between neighboring neurons. In mathematical terms, this can be written as the convolution ($\otimes$) of the present map activity a_{map} with an eye velocity weighted connectivity kernel (CK) as follows:

$$I = \left[CK \otimes a_{\text{map}}\right]^+ \tag{7}$$

$$\text{with } CK = c \cdot EV\,(t) \cdot M \tag{8}$$

$$\text{and } M = \begin{pmatrix} 1 & 0 & -1 \end{pmatrix} \tag{9}$$

M had the form of an edge detection filter, which was equivalent to computing the gradient. In other words, we computed the map's activity gradient and used the positive result (weighted by eye velocity) to update the neural activity in the map, i.e. to spread the activity. Neural activity gradients have been used previously to update retinotopic memory maps (Droulez and Berthoz, 1988; Droulez and Berthoz, 1991). Furthermore, eye/head position or velocity modulation of synaptic gains is believed to be a fundamental neural process in the brain (Salinas and Thier, 2000; Salinas and Sejnowski, 2001; Chance et al., 2002; Salinas, 2003). This synaptic gain modulation corresponds to a functional representation, not necessarily a proposed mechanism, and might involve other cells or circuits to be implemented. Here, the velocity weighted connectivity kernel implements such a gain modulation mechanism. Note that the exact shape of the kernel M was not important. Other asymmetric kernels provided similar results (data not shown). The constant c was adjusted to make the distance between neurons 1 deg and also provided the possibility to account for the variability of the subject's overall compensation gain.

The self-excitation input E (Fig. 4A) allowed the neural map to maintain its activity (Wang, 2001). Furthermore, we implemented a particular instance of a center-surround inhibitory mechanism (Salinas, 2003). Its goal was to allow the system to increase activity contrast in the neural map.

Therefore, we used a reverberation gain that depended on the position of maximum map activity:

$$k = k_0 + (1 - k_0) \cdot gauss\,(\mu, \sigma) \tag{10}$$

where k_0 was a constant reverberation gain (= minimal baseline feedback gain, Fig. 4B) parameter, μ was the position of the maximum map activity and $\sigma = 2$ and thus $E = k \cdot a_{\text{map}}$ (Fig. 4A). It is important to note that μ changes over time, because the activity maximum moves as the map activity spreads. This choice of the self-excitation gain resulted in a position dependent apparent time constant for the map's activity decay. That is, if eye velocity was zero, the relaxed form of Eq. (6) (with $I = 0$) yielded an apparent time constant $T_a = \frac{T_N}{1-k}$. Figure 4B shows the behavior of the apparent map dynamics as a function of the distance of the neuron from the location of the map maximum activity for the case $k_0 = 0.99$.

Finally, the read-out of the map assumed dynamics similar to the rate code mechanism above, i.e. accumulating evidence for the smooth eye displacement estimate. Again, this form of read-out was chosen to fit the delay between the smooth eye movement and the compensation for it observed in the data (Blohm et al., 2003; Blohm et al., 2005). The estimate of the instantaneous smooth eye displacement was computed using the center of activity (COA) of the displacement map (Fig. 4C).

$$T_{RO} \cdot \frac{d\text{SED}_{\text{est}}\,(t)}{dt} = -\text{SED}_{\text{est}}\,(t) + \text{COA}\,(t) \tag{11}$$

where $COA(t)$ was the activity weighted average of the neural map position x_i and T_{RO} was the time constant of the read-out neuron's activity (cf. rate code mechanism).

$$\text{COA}\,(t) = \frac{\sum_{\text{i=1}}^{\text{N}} a_{\text{map},i} \cdot x_i}{\sum_{\text{i=1}}^{\text{N}} a_{\text{map},i}} \tag{12}$$

We used the center of activity of the map because it is more insensitive to system noise than the activity maximum. There were thus three free parameters for the place code mechanism, i.e. the read-out time constant T_{RO}, the minimal baseline feedback gain k_0 and the gain constant c.

Behavioral experiments

We used an experimental behavioral data set from human subjects to fit the model's parameters. This experiment used ongoing smooth pursuit eye movements for the first "step" displacement in a "smooth double-step" paradigm. The paradigm and data were described in detail elsewhere (Blohm et al., 2005) and are summarized in Fig. 5. Briefly, the paradigm used a green initial fixation target that was presented for 500 ms at a random position on a 20° radius circle (Fig. 5A). Afterwards, the target stepped away from the center of the screen and moved at a random velocity (10°/s–40°/s) in the radial direction towards the center of the screen. At a random time 500–1500 ms after the ramp movement onset, a red target was briefly presented (10 ms flash) at a position horizontally and vertically offset from the actual green pursuit target location by a random value between − 10° and 10°. The pursuit ramp movement continued until the end of the trial that lasted for three seconds. Subjects were instructed to follow the green pursuit target and to look at the memorized position of the flash as soon as they saw the flash.

We provide some typical examples of subject's performance in Fig. 5B-F. Figure 5 shows position (panel B), velocity (panel C) and a spatial representation (panel D) from one trial. In this particular example, the first saccade was triggered shortly after the flash (latency = 104 ms). The black, dotted line indicates the line from the eye to the target at the time it was flashed. The red dotted line is the subsequent saccade, which is nearly parallel to the black line, indicating that the first saccade did not compensate for the smooth pursuit movement during the latency period of the saccade. A second saccade then brought the eye to the target. We show two other typical trials in Fig. 5E and F with longer latencies before the first saccade (panel E: 238 ms; panel F: 674 ms). The longer the latency to the first saccade, the more the saccade compensates for the smooth eye displacement in the latency period, and the less its trajectory parallels the black dotted line.

Hereafter, we will only present data from the time period of interest, i.e. starting at the moment of target presentation (10 ms flash) until 1000 ms after the flash presentation. This memory period included from 1 to 5 orientating saccades. For clarity, we decompose the two-dimensional saccade into components along, and perpendicular to, the direction of pursuit. Saccadic compensation for the smooth component of the eye movement took place mostly in the direction of the actual pursuit eye movement. Thus, below we keep only the component in the direction of pursuit, and consider the data as one dimensional.

To fit the eye velocity integration mechanisms described above to our data, we used the position error sampled at the moment of the flash occurrence (PE_{F}) along with the measured smooth eye velocity (EV) from the moment of the flash until the end of the simulation time. In addition, we also used the measured latencies of the orientating saccades as an input to the model (see Discussion section for further explanation). In order to evaluate the model parameters, we compared the predicted saccade amplitudes with those experimentally observed.

Simulations of data from the literature

At the end of the results section, we reproduce the data from Herter and Guitton (1998) and from McKenzie and Lisberger (1986) shown in Fig. 1. For the smooth eye velocity starting at the moment of the flash presentation and the saccade latencies measured with respect to the flash offset we used the following (idealized) functions:

McKenzie and Lisberger (1986):

$$EV(t) = \pm 30^\circ/s \cdot \left(1 - \frac{1}{1 + \exp\left(-\frac{t-0.3}{0.03}\right)}\right) \tag{13}$$

$$T_{\text{latency}} = Gauss\,(0.18, 0.045) \tag{14}$$

Herter and Guitton (1998):

$$EV(t) = \pm 15^\circ/s \cdot \left(1 - \frac{1}{1 + \exp\left(-\frac{t-0.3-T_{SP}}{0.03}\right)}\right) \tag{15}$$

$$T_{\text{latency}} = Gauss\,(T_{SP} + 0.25, 0.05) \tag{16}$$

The saccade latencies for the reconstruction (Eq. (14)) of McKenzie and Lisberger's data was a Gaussian distribution using the parameters from monkeys D and E (McKenzie and Lisberger, 1986); the smooth eye velocity (Eq. (13)) started decaying around 150 ms after the flash presentation as a sigmoid function. We used a similar smooth eye velocity profile to simulate Herter and Guitton's data (Eq. (15)), but now the

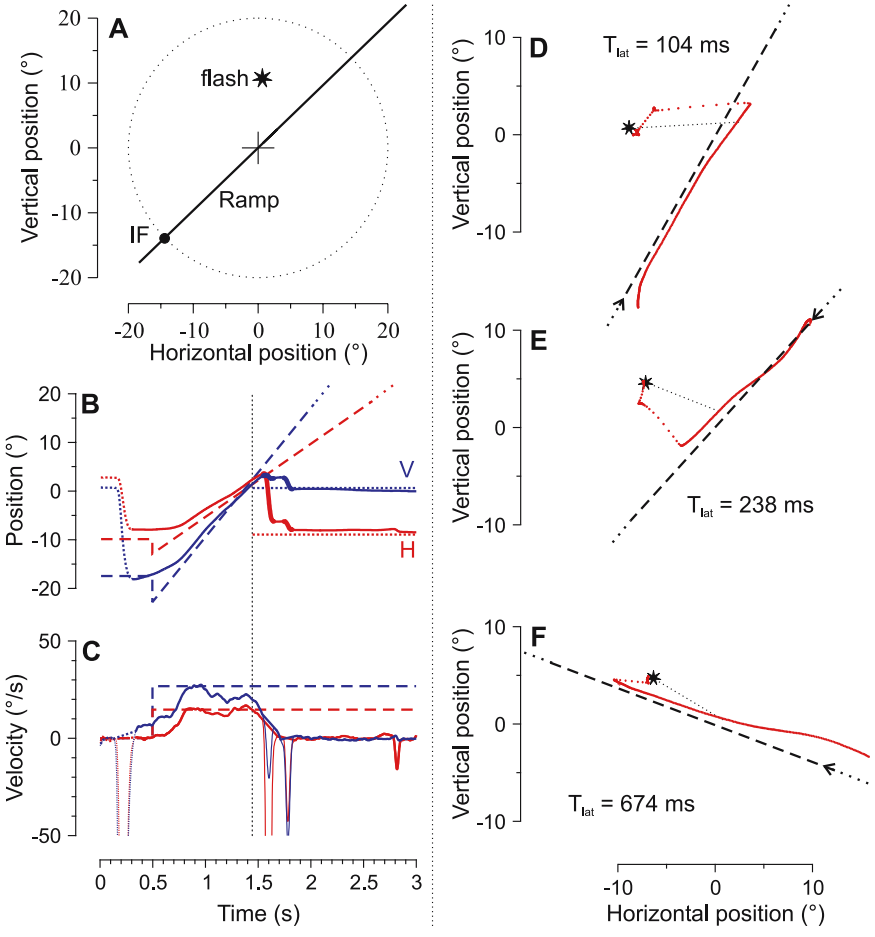

Fig. 5 Experimental data set used. (A). Paradigm. After an initial fixation (IF) at a random position of a 20° diameter circle (dotted), the green target moved (Ramp) at a random speed (10°/s–40°/s) towards the center of the screen (cross). At a random time after the target movement onset, another red target was flashed (10 ms, star) at a random position ± 10° around the current ramp position. Subjects were instructed to pursue the green ramp target and to saccade towards the memorized position of the flash as soon as possible. (B–D). Typical trial. Position (panel B) and velocity (panel C) traces of target (dashed) and eye (solid) for the horizontal (red) and vertical (blue) eye movement component. The horizontal and vertical dotted lines represent the moment of the flash presentation and the memorized position of the flash respectively. Panel D is a 2-dimensional representation of the eye (red dots, 6 ms spacing) and target (dashed) movement. The latency of the first saccade was 104 ms. (E). Another trial with a longer first saccade latency: 238 ms. (F). A trial with a very long first saccade latency: 674 ms. Figure modified from (Blohm et al. 2005)

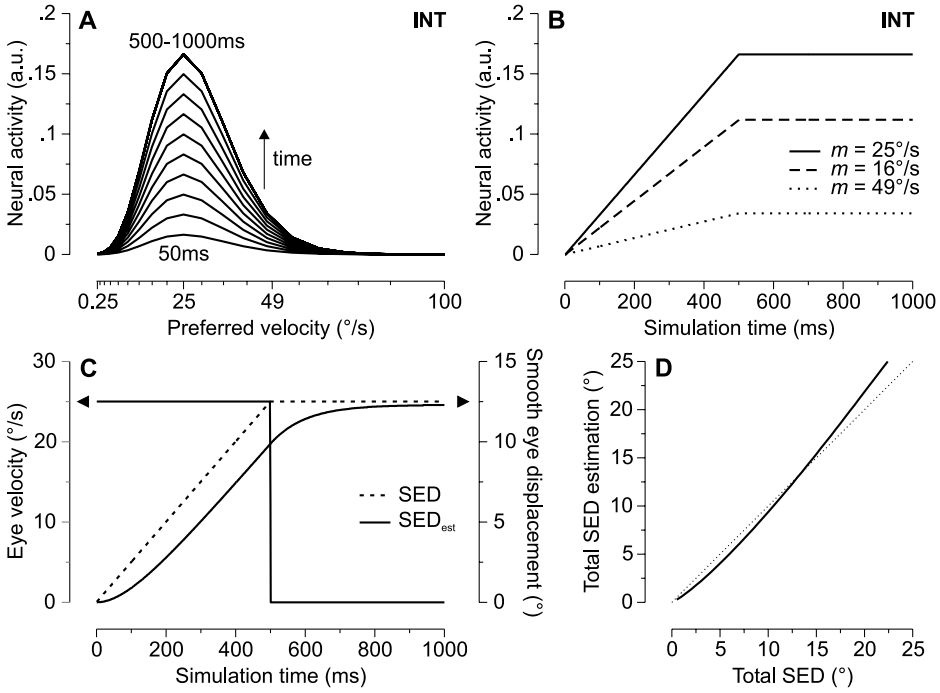

Fig. 6 Simulation results for the rate code mechanism. For this simulation, we used a read-out time constant $T_{RO} = 100$ ms and an accumulation gain $c = 0.5$. (A). Integration cell activity for different simulation times (50 ms step) between 50 ms and 1000 ms. Neurons were arranged in increasing order of preferred velocity. Simulations were performed with a 500 ms duration 25°/s eye velocity step. (B). Three examples of integration cell activity over time for different preferred velocity pathways (16, 25 and 49°/s). **(C).** Eye movement and estimation of the smooth eye displacement. The solid gray line was the eye velocity input used (left scale). The dotted black line corresponds to the actual smooth eye displacement and the solid black line was the model estimation of SED (right scale). (D). Estimation of the final SED as a function of the actual SED. The dotted line indicates the desired relationship. The solid line corresponds to the measured (slightly non-linear) model behavior. Simulations were performed with various 500 ms duration step-shaped eye velocities. The total duration of simulations was 1,000 ms

duration of the ramp (T_{SP}) was taken into account, since the target was flashed before the ramp onset. For the saccade latencies (Eq. (16)), we used a standard latency distribution as typically observed in human subjects (Becker, 1991; Carpenter and Williams, 1995), also taking into account the pursuit ramp duration (T_{SP}).

Results

The proposed rate and place code mechanisms were applied to the data separately. We will first describe the basic dynamics for each mechanism and fit the model parameters to the experimental data set. Afterwards, we will provide some examples of both smooth eye displacement estimation mechanisms. Finally, we will test our model by comparing it to the major findings of published experiments. We will reconcile previous contradictory data from the literature by reproducing all of the results with simulations of our model.

Analysis of the rate code mechanism

First, we analyzed the behavior of the rate code mechanism using default parameters (no fit to the data). Figure 6 shows the behavior of the rate code mechanism (2nd layer neurons) with parameters $T_{RO} = 100$ ms and $c = 0.5$ for a 500-ms test eye velocity input of 25°/s. For the sake of clarity, we arranged the neurons in increasing order of their tuning curve preferred velocity m in panel A. It can easily be seen that the activity of individual neurons rose linearly over time (Fig. 6B). Furthermore, the instantaneous read-out of the smooth eye displacement estimate was delayed with respect to the effective SED (Fig. 6C), because the dynamics of the accumulation of evidence for the read-out of neural activity were governed by T_{RO}. Finally, Fig. 6D shows that the model provided a good estimate of the smooth eye displacement up to about 20° of SED.

We fit the model to the observed behavior by identifying the optimal parameters for the rate code mechanism from experimental data. We varied the read-out time constant $T_{RO} = [1; 50; 100; 150; 200; 250; 300; 350; 400]$ ms and computed the model prediction of the experimental data for all saccades in each trial. The model's gain constant c was evaluated for each value of T_{RO} using a step eye velocity profile similar to the one used in Fig. 6C but varying the magnitude of eye velocity (as in Fig. 6D). The gain constant c was then adapted to provide a regression slope of 1 for the comparison between the estimation of SED and the actual SED generated

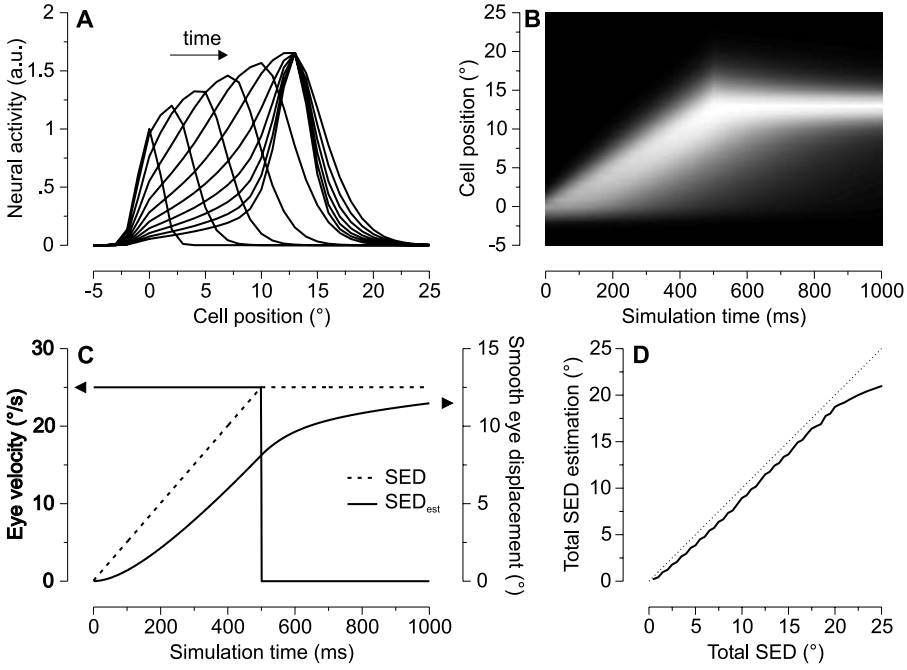

Fig. 7 Simulation results for the place code mechanism. For this simulation, we used a read-out time constant $T_{RO} = 100$ ms, a reverberation gain constant $k_0 = 0.99$ and an accumulation gain $c = 2.3$. (A). Activity of the neural map at different simulation times (50 ms step) ranging from 0 to 1000 ms. Each cell increment corresponded to 1° on the displacement map. Simulations were performed with a 500 ms duration 25°/s eye velocity step. (B). Evolution of neural activity in the displacement map over time (normalized activity; black = no activity; white = maximum activity). At time = 0 ms, the neural activity is maximal around zero displacement. With increasing time, the activity spreads towards neurons coding larger displacements, and there is remaining activity for neurons coding smaller positions. After the eye velocity drops (time > 500 ms), the spatial distribution of neural activity becomes narrower due to the center-surround modulation of the reverberation gain (Eq. (10)). (C). Eye movement and estimation of the smooth eye displacement. (D). Estimation of the final SED as a function of the actual SED. For panels C and D, the same conventions as for Fig. 6 apply

by the test eye velocity trace. Afterwards, we simulated the system's response to the flash stimulus using eye velocity, flash stimulus location and timing information concerning the compensatory saccades from data. There were $N = 4{,}464$ experimental trials with a total of $N = 9{,}150$ saccades. As an indicator of the goodness-of-fit of the model's prediction, we used the correlation coefficient R between the predicted and observed saccade amplitudes. Since there were no local maxima in the correlation coefficient, we chose the value with the absolute maximum of R as the optimal value of T_{RO}, i.e. 100 ms ($c = 0.493$, $R = 0.943$) for our trials. These values were used hereafter for all simulations of the rate code model.

Analysis of place code mechanism

Next, we analyzed the theoretical behavior of the place code mechanism. Figure 7 shows the results of this investigation for $T_{\mathrm{RO}} = 100$ ms, $c = 2.3$ and $k_0 = 0.99$. Figure 7A and B show the evolution of the map's neural activity over time as a response to the 500 ms duration step eye velocity profile of 25°/s. It can easily be observed that eye velocity "pushed" the map's activity to cells that code larger displacements. Furthermore, the center-surround mechanism sharpened the locus of activity. Indeed, the neural activity surrounding the activity maximum decreased over time. This led to a smooth eye displacement estimate that was delayed and low-pass filtered with respect to the actual SED (Fig. 7C). In addition, the estimated SED was almost linear with respect to the actual SED and the estimation gain was close to unity up to about 20° of SED (Fig. 7D). Thus, as was the case for the rate code mechanism, the place code mechanism provided a good estimate of the actual smooth eye displacement and introduced the delay necessary to simulate the experimental data.

Next, we identified the optimal parameters for the place code velocity integration mechanism to fit the experimental data. As we did for the rate code mechanism, we varied the read-out time constant $T_{RO} = [1; 50; 100; 150; 200; 250; 300; 350; 400]$ ms and the reverberation parameter $k_0 = [0.9; 0.975; 0.99; 0.995; 0.999]$ independently and evaluated the optimal gain constant c for each couple (T_{RO}, k_0). The reverberation parameters corresponded to the apparent neural time constant $T_a = [30; 60; 120; 300; 600; 3000]$ ms. Next, we compared the simulation data from each parameter pair (T_{RO}, k_0) with the experimental data. We measured the performance of the model compared to the experiment by computing the

correlation coefficient R between the simulated and behavioral saccades for each pair (T_{RO}, k_0). The optimal set of parameters (where R was maximal: $R = 0.958$) was $T_{RO} = 100$ ms, $k_0 = 0.975$ ($T_a = 120$ ms) and $c = 2.427$.

Comparison with experimental data

To illustrate the performance of our model, Fig. 8 shows three comparisons between simulation and experiment for short latency first saccades (panel A), long latency first saccades (panel B) and very long latency first saccades (panel C). The solid black line is the experimental data, and simulations from the rate code (solid red) and the place code (dashed green) models are almost perfectly superimposed. The remaining error was a combination of SED underestimation (due to the integration mechanism) and remaining PE_R due to the saccadic undershoot strategy. The proportion of uncompensated retinal position error PE_R was always 0.1^n, where n was the total number of saccades.

To provide a quantitative comparison between the simulation results of both the rate code and the place code mechanisms and the behavioral findings of a previous experimental study (Blohm et al., 2005), we analyzed the main effect of compensatory saccades. We used the SED compensation index CI, previously defined for the analysis of our experimental data (see Blohm et al., 2005) to quantify the SED compensation of each saccade leading to a remaining position error (PE) as follows:

$$CI = 1 + \frac{\text{PE}}{\text{SED}} \tag{17}$$

CI was calculated after each saccade and indicates which proportion of the actual SED was compensated. We calculated CI for up to 5 saccades within each trial (see Methods section). Figure 9 shows the results of this analysis for both the rate code (panel A) and the place code (panel B) eye velocity integration mechanisms. As can be observed, the simulation results fitted the behavior of CI for the data very well.

We also tested both the rate code and the place code mechanisms on previous findings reported in the literature and summarized in Fig. 1. First, we reproduced artificially the experimental stimulus configurations (see Methods section) as described in McKenzie and Lisberger (1986) and in Herter and Guitton (1998) and performed simulations of these experiments with our rate code and place code eye velocity integration mechanisms using the above-identified model parameters. The results of our simulations are shown in Fig. 10 where we overlaid simulations on the experimental data from Fig. 1 (data in black, rate code model in red, place code model in green). Clearly, our model provides an accurate prediction of the previously published data, although we did not use these data to fit the model parameters. Thus, this validates our model and reconciles previously contradictory findings.

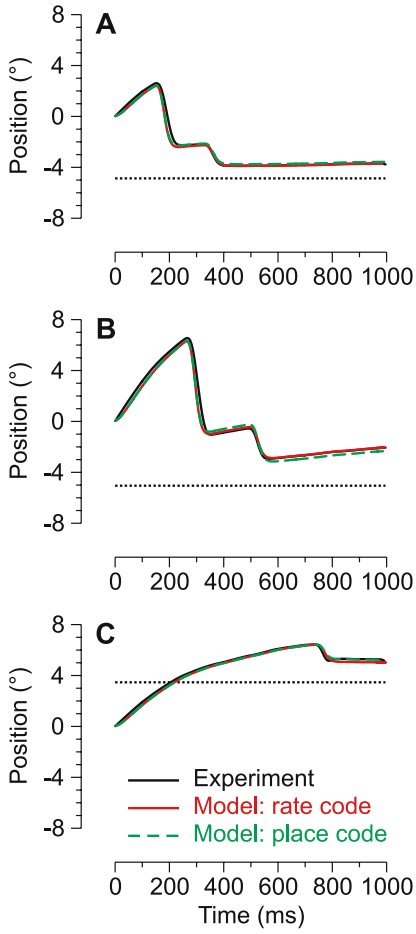

Fig. 8 Typical examples of comparison between simulations and experimental data. Panels A – C show three trials for different first saccade latencies (short, long and very long). Solid black lines are data, solid red lines correspond to rate code simulations and dashed green lines represent place code simulation results. Time 0 ms was the moment of target presentation (brief flash). (A). 1st saccade latency = 165 ms. (B). 1st saccade latency = 277 ms. (C). 1st saccade latency = 759 ms

Discussion

Contradictory results have been reported in the literature concerning the programming of the first saccade towards the memorized stimulus location when a smooth eye movement occurs after a target has been flashed. Whereas some studies reported retinotopically coded saccades (McKenzie and Lisberger, 1986; Gellman and Fletcher, 1992), other results favored spatially coded saccades (Schlag et al., 1990; Ohtsuka, 1994; Zivotofsky et al., 1996; Herter and Guitton, 1998; Baker et al., 2003). Recent data (Blohm et al., 2003; Blohm et al., 2005) suggested that these contradictory results

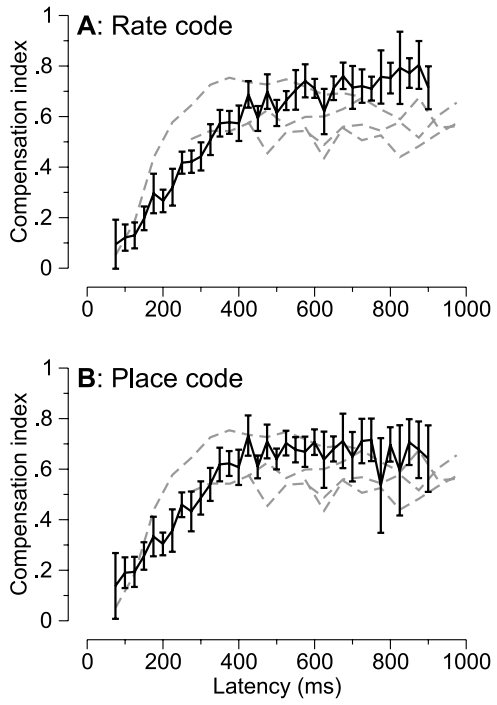

Fig. 9 Comparison between simulation data and experimental results. Comparison between the SED compensation index (*CI*, Eq. (13)) for experimental data (Blohm et al., 2005) (dashed gray lines stand for results from saccades 1 to 4) and simulation (black solid line) using the rate code mechanism (panel A) and the place code mechanism (panel B). Lines and whiskers stand for mean and 95% confidence intervals

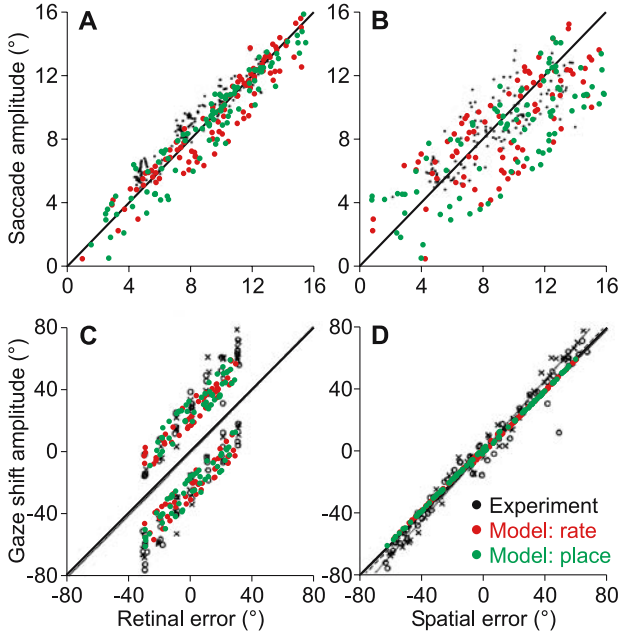

Fig. 10 Validation of the model based on the prediction of previously published experimental data. All panels correspond to the examples shown in Fig. 1. (A, B). Adapted from McKenzie and Lisberger (1986). C, D. Adapted from Herter and Guitton (1998). Rate code simulation data (red dots) and place code simulation data (green dots) were laid over the data from the literature (black symbols)

could be reconciled if one considered that the retinal to spatial transformation of the memorized target was a relatively slow process. Here, we tested that hypothesis. We proposed a saccade model that accounted for smooth eye movements in the absence of vision. We showed that two alternative mechanisms, i.e. a place code and a rate code mechanism, could both integrate a smooth eye velocity signal. Such a mechanism could provide an estimate of the smooth eye displacement (SED) to the posterior parietal cortex (PPC), a structure involved in the spatial representation of visual stimuli. SED signals could then be used by PPC to update the spatial representation of the target in eye-centered coordinates.

The proposed rate code SED estimation mechanism was based on an integration of the time during which the eyes moved at a specific velocity. The alternative place code mechanism was based on an eye velocity driven spread of neural activity on a topographic eye displacement map. Both mechanisms provided excellent simulations of our available test data set for "smooth double-step" experiments. Note that the fit of the simulations to the data was very accurate despite the small number of free parameters of the velocity integration mechanisms (1 for the rate code and 2 for the place code mechanism). Furthermore, our model could explain previously reported data and reconcile contradictory results.

General model discussion

Both smooth eye displacement estimation mechanisms proposed here used a high-gain, low-pass filtered, read-out of neural activity. This yielded the delay between the actual eye movement and the saccadic compensation found experimentally (Blohm et al., 2003, 2005). A reasonable rationale for such a delay process might be the system's need to ensure accuracy of the SED estimate. Low-pass filtering of the read-out of the integrative mechanism would reduce the influence of brief perturbations and system noise on the estimated SED. Therefore, reasonable amounts of white noise added to the individual neurons involved in the proposed mechanisms will not influence the outcome of the distributed SED integration process.

In the model presented here, no "pure" delay that could take into account the system's processing time has been implemented. However, once the decision to make a saccade has been made by the system, a processing time of approximately 50 ms (Thier and Andersen, 1996; Mushiake et al., 1999) is necessary to generate the final motor command and send it to the extraocular muscles. This delay was included implicitly in the activity read-out time constant we estimated for both mechanisms from our data sets. Consequently, we overestimated the read-out constant for the SED estimation.

In contrast to a standard read-out delay in either mechanism, one could imagine that the oculomotor system might use some kind of a threshold function instead. In other words,

the system might adapt the saccade amplitude or trigger a corrective saccade each time a certain smooth eye displacement has been accumulated. However, such a threshold mechanism makes several predictions. First, for large changes in SED (i.e., high smooth eye velocity), the mean saccade latency should be less than for small changes in SED. However, this was not found in the experimental data. Blohm et al. (2005) actually found that the opposite was the case, i.e. the system waited longer when the smooth eye movement was large. Second, a threshold mechanism would not be able to account for the delay between the actual smooth eye movement and the saccadic compensation for it. Once the threshold is reached, a saccade would be triggered that would compensate for all the SED accumulated until the saccade and thus there would be no delay in the compensation measured. Third, the amplitude of corrective saccades should be very stereotypical and equal to the hypothetical threshold value. Again, this has not been observed experimentally. Instead, the amplitude of the corrective saccades was very variable (Blohm et al., 2003, 2005). These results make it unlikely that the oculomotor system uses a threshold mechanism.

For each model, we evaluated theoretically the optimal gain constant c before fitting the simulations to the experimental data. As a consequence, this procedure assumed that at simulation time infinity, the compensation for the smooth eye movement was perfect (see Fig. 1D). In contrast with this hypothesis, the available experimental results suggested that subjects might underestimate the actual SED up to 50% (Blohm et al., 2003, 2005). However, as shown in Fig. 9 and 10 our model fits the data despite the apparent contradiction between the choice of the model gain constant c and the measured final SED compensation gain. We believe that the underestimation of SED in the data was (at least partially) due to the finite number of corrective saccades. That is, if the system triggered a saccade that compensated for the available SED but the eyes continued moving smoothly afterwards, then the final SED compensation gain would be <1.

Since we concentrated on the mechanism for extraretinal eye velocity integration, our model did not describe how the saccades might be triggered. Indeed, the mechanism that initiated those compensatory eye movements is largely unknown. For the first orienting saccade, Blohm et al. (2005) showed evidence for a trade-off between speed and accuracy, demonstrating that the system could use extraretinal information in addition to the known sensory input (de Brouwer et al., 2002b). But the precise mechanism to trigger these initial saccades has not yet been identified. This might at least partly be due to the fact that saccade latencies show a large natural variability (Becker, 1991; Carpenter and Williams, 1995; Reddi and Carpenter, 2000; Reddi et al., 2003). In addition to the trigger mechanism for the first saccade, compensatory saccades need to be triggered by some still unknown mechanism. However, the experimental data available today does reveal how compensation saccades are initiated. To illustrate the experimental variability of the successive saccade latency, we show in Fig. 11 the distribution of the time interval between saccades, i.e. the inter-saccadic interval (ISI). The inter-saccadic interval was not significantly modulated by eye velocity or smooth eye displacement (data not shown), nor was there a correlation with some displacement threshold (see Discussion above). Altogether, more research is needed to identify the decision processes that triggers the first saccade and the compensatory saccades, although some neural signals related to this decision have been observed (Hanes and Schall, 1996; Schall and Bichot, 1998; Schall and Hanes, 1998; Kim and Shadlen, 1999; Schall and Thompson, 1999; Gold and Shadlen, 2001; Schall, 2001; Roitman and Shadlen, 2002). Because none of the fundamental mechanisms that initiate a saccade are known today, we decided not to model the trigger mechanism but used the experimentally measured saccade occurrence time.

Model comparison with data

The model simulations closely fitted the experimental data set we used here (cf. Figs. 8 and 9). The amplitudes of all saccades occurring at different latencies with respect to the memorized target appearance was well predicted. In addition, we reproduced the main results for the smooth eye movement compensation index CI of individual saccades. The remaining, small differences between the model simulation and the experimental results might be due to the biological variability of saccades. In addition to the experimental data set we used here for the identification of the model parameters, we also tested our model on "smooth double-step" data using smooth anticipatory eye movements (Blohm et al., 2003). In this experiment, a robust anticipatory

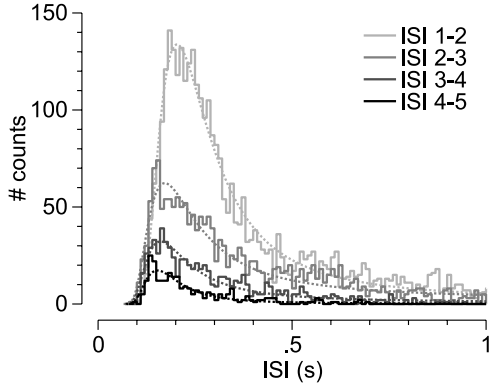

Fig. 11 Experimental results for the inter-saccadic interval (ISI). The distribution of time intervals between successive saccades is shown for up to 5 saccades. Solid histogram is raw data (10 ms bins), dotted lines are recinormal distribution fits

smooth eye movement was built up during repetitive tracking of the same moving stimulus. Then, Blohm et al. (2003) randomly replaced a few tracking trials by flash localization trials, where a target was briefly flashed in an eccentric position during an anticipatory smooth eye movement. Subjects were then asked to look at the memorized position of the flash. Doing so, Blohm et al. (2003) observed behavior very similar to that observed in the data set used to fit our rate code and place code mechanisms, despite the fact that subjects did not have any visual information at all about the smooth eye displacements. We also tested our model using this second data set (data not shown). First, we identified the model parameters that would fit the smooth anticipation data and found those to be the same as those identified for the above-described experimental data. Second, we tested our model's prediction of saccade amplitude of this anticipation data set and were able to reproduce the main effects reported in Blohm et al. (2003). This was an additional validation of our model.

We also tested our model on two representative data sets from the literature. Our simulations accurately reproduced data from Herter and Guitton (1998), showing that saccades to targets memorized before a pursuit eye movement were spatially accurate (Schlag et al., 1990; Ohtsuka, 1994; Zivotofsky et al., 1996; Herter and Guitton, 1998; Baker et al., 2003). Furthermore, previous findings on retinotopically programmed short latency saccades to memorized targets (McKenzie and Lisberger, 1986; Gellman and Fletcher, 1992) were also reproduced. The delay for SED estimation in our model reconciled those contradictory findings, i.e. short latency saccades were better predicted by the retinal error hypothesis than by the spatial error hypothesis.

This model is a valuable tool to analyze and interpret saccade data compensating for smooth eye movements. It has been shown recently that this compensation plays a crucial role during temporary occlusions of moving targets (Bennett et al., 2004). One prediction of our model concerns the saccades triggered during a transient extinction of a pursuit target (Bennett and Barnes, 2003). If the saccade latency were long enough (>300 ms), the amplitude of those saccades should be tightly related to the actual smooth eye displacement in darkness. This seemed to be the case for saccades reported by Bennett and Barnes (2003), even though no statement on saccade latency was made in their study.

Hypothesized neural substrates

General hypothesized neurophysiology

It is generally accepted that the posterior parietal cortex (PPC) is implicated in visual short-term memory and coordinate transformations for saccadic eye movements. Neurons in the lateral intraparietal area (LIP, PPC) remain active while a desired target location is remembered, i.e. they retain a memory of the motor error (Gnadt and Andersen, 1988; Barash et al., 1991; Paré and Wurtz, 1997; Curtis et al., 2004). Furthermore, electrical stimulation of some sites in LIP produces fixed vector saccades independent of eye position, whereas others encode saccades to targets in a specific spatial position (Thier and Andersen, 1996; Thier and Andersen, 1998). LIP neurons are influenced by eye position (Andersen et al., 1990b; Bremmer et al., 1997), and some cells show a shift in their response field that anticipates an upcoming gaze saccade (Duhamel et al., 1992a; Mushiake et al., 1999). In addition, LIP neurons discharge prior to saccades (Barash et al., 1991). Lesions of the human analog of LIP in PPC impair the ability to perform the double-step task, i.e. disrupt the monitoring of previous saccades by efference copy (Duhamel et al., 1992b; Heide et al., 1995). This shows the importance of PPC in the internal representation of targets in space (Tobler et al., 2001). Furthermore, humans with chronic PPC lesions make inaccurate memory guided saccades (Pierrot-Deseilligny et al., 1991). Moreover, area 7a (an area adjacent to LIP in the monkey's PPC) also contains neurons with eye and head position dependent activity that encode a visual target in spatial or craniotopic coordinates (Andersen et al., 1990b, 1992; Brotchie et al., 1995; Bremmer et al., 1997). Taken together, this evidence suggests that saccadic goals are memorized with respect to different reference frames (e.g. retinal and spatial) in PPC. When a gaze shift occurs, the retinotopic position of targets (Henriques et al., 1998; Medendorp et al., 2002; Merriam et al., 2003) is updated (Andersen et al., 1997; Colby and Goldberg, 1999) using extraretinal information about the gaze shift amplitude (Quaia et al., 1998). Therefore, we suggest that in the "smooth double-step" paradigm, PPC receives an internal estimation of the (smooth) eye displacement to update the spatial representation of the memorized goal. For smooth eye displacements, PPC could play a similar role in updating retinotopic information after receiving an estimate of pursuit eye displacement.

The studies about the target representation in spatial coordinates in PPC report that updates are performed on the basis of *position* signals representing the gaze shift amplitude. However, this implies that in the case of the "smooth double-step" paradigm, where eye *velocity* is monitored, there must be an additional step: the integration of eye velocity to obtain eye displacement. Thus, integration of eye velocity needs to take place before the updating of the spatial target representation in PPC. This integration step could be performed in a variety of different neural structures using either our rate code or place code mechanisms.

Hereafter, we will discuss the electrophysiological evidence that supports these alternatives.

Hypothesized neurophysiology of the rate code mechanism

The first smooth eye velocity integration mechanism we considered is based on an integration of ocular motion signals, and we suggest that this rate code mechanism could be implemented in area LIP. An area that contains neurons encoding eye velocity (the medial superior temporal cortex, MST) is known to project to LIP. Cells in MST are tuned selectively for visual motion and are modulated by extraretinal eye velocity signals (Komatsu and Wurtz, 1988a; Komatsu and Wurtz, 1988b; Newsome et al., 1988; Bradley et al., 1996; Squatrito and Maioli, 1997; Ilg and Thier, 2003) and project largely to LIP (Cavada and Goldman-Rakic, 1989; Andersen et al., 1990a; Neal et al., 1990). We hypothesize that some LIP neurons integrate the activity of eye velocity-sensitive MST cells. Neurons in LIP have been shown to monotonically increase their firing rate in response to time-varying signals that originate in the extrastriate visual cortex (in particular from the medial temporal cortex), thereby accumulating evidence for a specific behavioral response (Shadlen and Newsome, 1996; Roitman and Shadlen, 2002; Mazurek et al., 2003). The approximately linear neural activity of these LIP cells has also been related to a representation of elapsed time (Rao et al., 2001; Leon and Shadlen, 2003). In our rate-code integration hypothesis, one LIP neuron would receive an input from one MST neuron encoding eye velocity. The discharge of this LIP cell, if it acted as an integrator, would be proportional to the amount of time an eye movement had the preferred velocity of the specific MST neuron. The readout of this system is then the accumulation of the activity of each LIP neuron with a synaptic weight proportional to the preferred velocity of the corresponding MST neuron (displacement = time $*$ velocity). Thus, a weighted sum of all LIP activity is an estimate of the smooth eye displacement.

One way to test whether the rate code mechanism is responsible for the integration of extraretinal eye velocity signals would be to remove the source of extraretinal eye velocity signals by inactivating area MST. Despite a deficit in smooth pursuit, some smooth eye movements should persist (Dursteler et al., 1987). In addition, another possibility would be to use smooth anticipatory eye movements as has been done by Blohm et al. (2003). The advantage of using smooth anticipation is that these eye movements are believed to rely principally on cognitive cues and might be generated by the frontal cortex (Missal and Heinen, 2001, 2004). Another interesting experiment to identify the hypothesized integration neurons would be to record neurons in LIP that have previously been shown to carry time-related information (Rao et al., 2001; Leon and Shadlen, 2003). The activity of such LIP integration neurons should rise approximately linearly (in a "smooth double-step" paradigm) during the memory period after target presentation. The rate of rise of those neurons should be velocity tuned. This would be in accordance with previous findings demonstrating that many LIP neurons exhibit direction-specific activity during smooth pursuit and continue firing when the visual stimulus is intermittently turned off (Sakata et al., 1983; Bremmer et al., 1997).

As an alternative to LIP, the ventral intraparietal area (VIP) could also be involved in the integration of smooth eye velocity signals. VIP contains neurons responding to extraretinal velocity signals (Colby et al., 1993; Schlack et al., 2003) and receives extensive input from MST (Van Essen et al., 1981; Lewis and Van Essen, 2000). Furthermore, it has been shown that VIP neurons encode heading in head-centered coordinates and thus provide a reliable source of information about smooth motion (Bremmer et al., 2002; Zhang et al., 2004). Also, VIP has projections to LIP (Lewis and Van Essen, 2000) that could mediate the SED estimation signal to update the memorized target position. The activity and characteristics of those VIP cells is thus compatible with our hypothetical rate code mechanism. Another neural structure that could implement the rate code mechanism we propose here is the frontal eye field (FEF). FEF has large reciprocal projections with motion area MST (Ungerleider and Desimone, 1986; Tusa and Ungerleider, 1988) and contains separate saccadic and smooth eye movement regions (for a review, see Krauzlis, 2004). Neurons in FEF are known to show rising signals in preparation of a saccadic movement onset (Hanes and Schall, 1996; Schall and Bichot, 1998; Schall and Hanes, 1998; Schall and Thompson, 1999; Schall, 2001). Although this observation was attributed to the decision process of triggering a saccade, a similar mechanism could integrate eye velocity signals to compute the smooth eye displacement. This hypothesis is also supported by the finding that FEF can integrate velocity signals to extrapolate the position of an invisibly moving target (Barborica and Ferrera, 2003).

Hypothesized neurophysiology of the place code mechanism

The second smooth eye displacement estimation mechanism we consider is based on a place code mechanism, and the role of the cerebellum (CBLM) in monitoring eye movements suggests that this mechanism might be implemented by the cerebellum. We think that the cerebellum is a good candidate for the integration of eye velocity, since eye/gaze velocity signals are present in different cerebellar areas. Indeed, parafloccular (PF), floccular (Floc) and vermal Purkinje cells encode gaze velocity during smooth pursuit or combined eye-head tracking (Miles and Fuller, 1975; Lisberger and Fuchs, 1978a, b; Suzuki and Keller, 1988a, b;

Nagao et al., 1997). Also, the cerebellum is thought to be a crucial structure for the generation of smooth pursuit eye movements (for a review, see Krauzlis, 2004). In addition, recent models of the saccadic system interpret the function of the cerebellum as a controller that monitors ongoing eye movements by integrating velocity feedback signals to steer and stop the saccade (Lefèvre et al., 1998; Quaia et al., 1999; Optican and Quaia, 2002). In these models, eye velocity signals evoke a spread of activity on a topographically organized neural map. This spatial integration of velocity signals replaces temporal integration, i.e. the "displacement integrator" of classical models (Jürgens et al., 1981), and underlies our hypothesis that the cerebellum also contains a smooth eye displacement map. Such a map would enable the saccadic system to monitor smooth eye movements and allow the oculomotor system to ensure space constancy during smooth eye movements in darkness. The readout of this displacement map would then be sent from the cerebellum to LIP to update the spatial representation of the memorized target. Different direct and indirect projections from the cerebellum to LIP have been reported (Clower et al., 2001), as required by this hypothesis.

To identify the neural substrate of a possible role of the cerebellum in the integration of smooth eye velocity signals, different experiments using a "smooth double-step" paradigm could be performed. Our place code mechanism predicts the presence of a topological map within the cerebellum. Neurons within this map should code eye displacement. Furthermore, the gain of interconnection between these neurons should be modulated by eye velocity. We believe that the cerebellar cortex would be a good candidate for such a mechanism, because the theoretical behavior of our displacement map is compatible with the organization of the structure and the interconnection of the different types of neurons in the cerebellar cortex (Ghez and Thach, 2000).

We propose that the displacement map for eye velocity integration in our place code mechanism is implemented by part of the oculomotor cerebellum, such as the vermis (lobuli VI and VII) and the fastigial nucleus (FN)—one of the deep cerebellar nuclei (DCN)—to which the vermal Purkinje cells (P-cells) projects (Suzuki et al., 1981; Noda and Fujikado, 1987; Suzuki and Keller, 1988a, b; Takagi et al., 2000; Robinson and Fuchs, 2001). It is difficult, however, to speculate about how exactly the cerebellar cortex could implement the place code mechanism we propose here. Although the connectivity of the cerebellar cortex is well known (Eccles et al., 1967), its functional role and possible computations remain largely unidentified (Wolpert et al., 1998; Ghez and Thach, 2000). Nevertheless, from a connectionist point of view, all the required elements to implement our place code model mechanism are present: First, the fastigial nucleus (FN) could represent the read-out structure of the integrated eye velocity signal, i.e. the smooth eye displacement, since the fastigial nucleus and the inferior olivary nucleus (ION) form an inhibitory control loop that could implement the map activity weighting of the read-out we propose (Hoddevik et al., 1976; Buisseret-Delmas, 1988). Second, a smooth eye velocity efference copy signal is sent from the pre-cerebellar nuclei [dorsolateral pontine nucleus (Mustari et al., 1988; Thier et al., 1988; Krauzlis, 2004), dorsomedial pontine nucleus (Keller and Crandall, 1983; Krauzlis, 2004) and the nucleus reticularis tegmenti pontis (Crandall and Keller, 1985; Suzuki et al., 2003; Krauzlis, 2004)] to the glomeruli in the granular layer of the cerebellar cortex. Glomeruli form the input to granule cells and the granule cell's output (parallel fibers) project to golgi cells, which in turn inhibit the glomeruli (Eccles et al., 1967; Ghez and Thach, 2000). This circuit forms an inhibitory control loop that influences the signals in the parallel fibers—a major input to Purkinje-cells (the map neurons in our place code mechanism). Together with other Purkinje-cell inhibitors (stellate and basket cells) this part of the cerebellar connectivity could implement the eye velocity modulation of the Purkinje-cell activity and the center-surround modification of the reverberation gain in our place code mechanism. Third, the latter reverberation circuit might find its neural analogue in the excitatory P-cell-DCN-ION control loop (Eccles et al., 1967; Ghez and Thach, 2000).

Such a functional hypothesis remains, of course, highly speculative. It demonstrates, however, that the cerebellum has all the elements necessary to perform the eye velocity integration we propose here. Further research is needed to identify the computational role and flexibility of the cerebellar cortex. Alternatively, the ventral cerebellar paraflocculus (VPF) could also implement the displacement map for eye velocity integration we propose in our place code mechanism. Indeed, the ventral cerebellar paraflocculus has the same functional anatomy as the vermis and is also involved in smooth pursuit eye movement control (Rambold et al., 2002).

In addition to these predictions of neural activity in the cerebellum, SED information needs to be sent to area LIP in the parietal cortex. Some potential direct pathways have been identified (Clower et al., 2001), but their functional roles have not yet been investigated. An alternative candidate for a SED feedback pathway to LIP would be an indirect projection via the thalamus. The mediodorsal thalamus has been shown to play a role in the internal monitoring of movements by providing feedback about the amplitude of (saccadic) eye movements to the cortex (Sommer and Wurtz, 2002; Sommer, 2003; Sommer and Wurtz, 2004a, b;). A recent study has also reported that the central thalamus was involved in the control (and perhaps monitoring) of smooth pursuit eye movements

(Tanaka, 2005). This could be tested by recording from the thalamus and looking for signals related to SED during a "smooth double-step" paradigm.

Other considerations

In our model, we suppose that the rate or place code mechanisms update the memorized position of the target in PPC and that PPC in turn sends information about the amplitude of an upcoming saccade to FEF and SC. This would mean that SC must code the total saccade amplitude, including the smooth eye displacement component (if available to the system). However, smooth eye displacement information could also be sent in parallel to the SC pathway and to the saccade generator (situated downstream from SC), as seems to be the case for retinal slip signals in catch-up saccades (May et al., 1988; Thurston et al., 1988; Keller et al., 1996). The fastigial oculomotor region (FOR) in the cerebellum could mediate such a parallel pathway, which is a particularly interesting hypothesis for our place code smooth eye velocity integration mechanism, which we hypothesize may be implemented in the cerebellum. As a result of such an adaptation of saccade metrics in parallel to the SC pathway, the neural coding of the saccade amplitude in SC should not reflect any information about the smooth eye displacement. In contrast, the rate code mechanism (which we hypothesize may be implemented in LIP) would be more likely to have an effect on the coding of saccade amplitude in SC. This would be an interesting issue to test and could contribute to the discrimination between the proposed rate and place code mechanisms.

Finally, the origin of the eye velocity signals used to estimate SED needs to be identified. There are two candidates, i.e. motor command efference copy signals and muscle proprioceptive afference. Today, it seems unlikely that proprioceptive information is used in online control of eye movements (Ruskell, 1999; Weir et al., 2000; Lewis et al., 2001). However, until this issue has been addressed specifically, a possible role of proprioception in SED estimation cannot be excluded. Therefore, a "smooth double-step" experiment should be performed after deafferentation of the extraocular muscles in monkeys to answer this question.

A challenge of modeling neural processes is that predictions have to be made about both the underlying neural substrates and their functional roles. The two eye velocity integration mechanisms we proposed here are supported by current knowledge about their neural analogs, yet remain quite speculative. Nonetheless, they have everything a model needs: they are relatively simple, physiologically realistic and describe all available data. And in addition, they make interesting predictions about the neural substrates and signals and account for the current physiological knowledge of the structures modeled. Most importantly, our eye velocity integration model reconciles previously contradictory findings of retinally coded versus spatially accurate memory saccades during smooth pursuit eye movements. This first quantitative attempt explains the observed phenomena using physiologically inspired artificial neural networks to perform a delayed integration of velocity signals.

Acknowledgments This work was supported by the Fonds National de la Recherche Scientifique; the Fondation pour la Recherche Scientifique Médicale; the Belgian program on Interuniversity Attraction Poles initiated by the Belgian Federal Science Policy Office; internal research grant (Fonds Spéciaux de Recherche) of the Université catholique de Louvain. Gunnar Blohm is currently supported by a Marie Curie International fellowship within the 6th European Community Framework Program. Lance M. Optican is supported by the Intramural Research Program, NEI/NIH/DHHS. The scientific responsibility rests with its authors.

References

Andersen RA, Asanuma C, Essick G, Siegel RM (1990a) Corticocortical connections of anatomically and physiologically defined subdivisions within the inferior parietal lobule. J. Comp. Neurol. 296: 65–113.

Andersen RA, Bracewell RM, Barash S, Gnadt JW, Fogassi L (1990b) Eye position effects on visual, memory, and saccade-related activity in areas LIP and 7a of macaque. J. Neurosci. 10: 1176–1196.

Andersen RA, Brotchie PR, Mazzoni P (1992) Evidence for the lateral intraparietal area as the parietal eye field. Curr. Opin. Neurobiol. 2: 840–846.

Andersen RA, Snyder LH, Bradley DC, Xing J (1997) Multimodal representation of space in the posterior parietal cortex and its use in planning movements. Annu. Rev. Neurosci. 20: 303–330.

Aslin RN, Shea SL (1987) The amplitude and angle of saccades to double-step target displacements. Vision Res. 27: 1925–1942.

Baker JT, Harper TM, Snyder LH (2003) Spatial memory following shifts of gaze. I. Saccades to memorized world-fixed and gaze-fixed targets. J. Neurophysiol 89: 2564–2576.

Barash S, Bracewell RM, Fogassi L, Gnadt JW, Andersen RA (1991) Saccade-related activity in the lateral intraparietal area. II. Spatial properties. J. Neurophysiol 66: 1109–1124.

Barborica A, Ferrera VP (2003) Estimating invisible target speed from neuronal activity in monkey frontal eye field. Nat. Neurosci. 6: 66–74.

Becker W (1991) Saccades. In: Carpenter R, ed. Eye Movements MacMillan Press, Houndmills, UK, pp. 95–137.

Becker W, Jürgens R (1979) An analysis of the saccadic system by means of double step stimuli. Vision. Res. 19: 967–983.

Bennett SJ, Barnes GR (2003) Human ocular pursuit during the transient disappearance of a visual target. J. Neurophysiol 90: 2504–2520.

Bennett SJ, Barnes GR, Orban de Xivry J-J, Lefèvre P (2004) Ocular pursuit to a predictable velocity and/or position change during the occlusion of a moving target. In: Annual Meeting of the Society for Neuroscience, vol Program No. 712.6. 2004 Abstract Viewer/Itinerary Planner, San Diego.

Blohm G, Missal M, Lefèvre P (2003) Interaction between smooth anticipation and saccades during ocular orientation in darkness. J. Neurophysiol. 89: 1423–1433.

Blohm G, Missal M, Lefèvre P (2005) Processing of retinal and extraretinal signals for memory-guided saccades during smooth pursuit. J. Neurophysiol. 93: 1510–1522.

Bradley DC, Maxwell M, Andersen RA, Banks MS, Shenoy KV (1996) Mechanisms of heading perception in primate visual cortex. Science 273: 1544–1547.

Bremmer F, Distler C, Hoffmann KP (1997) Eye position effects in monkey cortex. II. Pursuit- and fixation- related activity in posterior parietal areas LIP and 7A. J. Neurophysiol. 77: 962–977.

Bremmer F, Duhamel JR, Ben Hamed S, Graf W (2002) Heading encoding in the macaque ventral intraparietal area (VIP). Eur. J. Neurosci. 16: 1554–1568.

Brotchie PR, Andersen RA, Snyder LH, Goodman SJ (1995) Head position signals used by parietal neurons to encode locations of visual stimuli. Nature 375: 232–235.

Buisseret-Delmas C (1988) Sagittal organization of the olivocerebellonuclear pathway in the rat. I. Connections with the nucleus fastigii and the nucleus vestibularis lateralis. Neurosci. Res. 5: 475–493.

Carpenter RH, Williams ML (1995) Neural computation of log likelihood in control of saccadic eye movements [see comments]. Nature 377: 59–62.

Cavada C, Goldman-Rakic PS (1989) Posterior parietal cortex in rhesus monkey: I. Parcellation of areas based on distinctive limbic and sensory corticocortical connections. J. Comp. Neurol. 287: 393–421.

Chance FS, Abbott LF, Reyes AD (2002) Gain modulation from background synaptic input. Neuron. 35: 773–782.

Cheng K, Hasegawa T, Saleem KS, Tanaka K (1994) Comparison of neuronal selectivity for stimulus speed, length, and contrast in the prestriate visual cortical areas V4 and MT of the macaque monkey. J. Neurophysiol. 71: 2269–2280.

Clower DM, West RA, Lynch JC, Strick PL (2001) The inferior parietal lobule is the target of output from the superior colliculus, hippocampus, and cerebellum. J. Neurosci. 21: 6283–6291.

Colby CL, Duhamel JR, Goldberg ME (1993) Ventral intraparietal area of the macaque: anatomic location and visual response properties. J. Neurophysiol. 69: 902–914.

Colby CL, Goldberg ME (1999) Space and attention in parietal cortex. Annu. Rev. Neurosci. 22: 319–349.

Crandall WF, Keller EL (1985) Visual and oculomotor signals in nucleus reticularis tegmenti pontis in alert monkey. J. Neurophysiol. 54: 1326–1345.

Curtis CE, Rao VY, D'Esposito M (2004) Maintenance of spatial and motor codes during oculomotor delayed response tasks. J. Neurosci. 24: 3944–3952.

Dassonville P, Schlag J, Schlag-Rey M (1992) The frontal eye field provides the goal of saccadic eye movement. Exp. Brain Res. 89: 300–310.

de Brouwer S, Missal M, Barnes G, Lefèvre P (2002a) Quantitative analysis of catch-up saccades during sustained pursuit. J. Neurophysiol. 87: 1772–1780.

de Brouwer S, Missal M, Lefèvre P (2001) Role of retinal slip in the prediction of target motion during smooth and saccadic pursuit. J. Neurophysiol. 86: 550–558.

de Brouwer S, Yuksel D, Blohm G, Missal M, Lefèvre P (2002b) What triggers catch-up saccades during visual tracking? J. Neurophysiol. 87: 1646–1650.

DeAngelis GC, Uka T (2003) Coding of horizontal disparity and velocity by MT neurons in the alert macaque. J. Neurophysiol. 89: 1094–1111.

Dominey PF, Schlag J, Schlag-Rey M, Arbib MA (1997) Colliding saccades evoked by frontal eye field stimulation: artifact or evidence for an oculomotor compensatory mechanism underlying double-step saccades? Biol. Cybern. 76: 41–52.

Droulez J, Berthoz A (1988) Spatial and temporal transformations in visuo-motor coordination. In: Eckmiller R, van den Malsburg C, eds. Neural Computers, vol F41. Springer, Berlin, pp. 345–357.

Droulez J, Berthoz A (1991) A neural network model of sensoritopic maps with predictive short-term memory properties. Proc. Natl. Acad. Sci. USA 88: 9653–9657.

Duhamel JR, Colby CL, Goldberg ME (1992a) The updating of the representation of visual space in parietal cortex by intended eye movements. Science 255: 90–92.

Duhamel JR, Goldberg ME, Fitzgibbon EJ, Sirigu A, Grafman J (1992b) Saccadic dysmetria in a patient with a right frontoparietal lesion. The importance of corollary discharge for accurate spatial behaviour. Brain 115: 1387–1402.

Dursteler MR, Wurtz RH, Newsome WT (1987) Directional pursuit deficits following lesions of the foveal representation within the superior temporal sulcus of the macaque monkey. J. Neurophysiol. 57: 1262–1287.

Eccles JC, Ito M, Szentagothai J (1967) The cerebellum as a neural machine. Springer, Berlin, Heidelberg, New York.

Felleman DJ, Kaas JH (1984) Receptive-field properties of neurons in middle temporal visual area (MT) of owl monkeys. J. Neurophysiol. 52: 488–513.

Gellman RS, Carl JR (1991) Motion processing for saccadic eye movements in humans. Exp. Brain Res. 84: 660–667.

Gellman RS, Fletcher WA (1992) Eye position signals in human saccadic processing. Exp. Brain Res. 89: 425–434.

Ghez C, Thach WT (2000) The Cerebellum. In: ER Kandel, JH Schwartz, Jessell TM, eds. Principles of Neural Science, McGraw-Hill, Nex York, pp. 832–852.

Gnadt JW, Andersen RA (1988) Memory related motor planning activity in posterior parietal cortex of macaque. Exp. Brain Res. 70: 216–220.

Gold JI, Shadlen MN (2001) Neural computations that underlie decisions about sensory stimuli. Trends Cogn. Sci. 5: 10–16.

Goossens HH, Van Opstal AJ (1997) Local feedback signals are not distorted by prior eye movements: Evidence from visually evoked double saccades. J. Neurophysiol. 78: 533–538.

Hallett PE, Lightstone AD (1976a) Saccadic eye movements to flashed targets. Vision Res. 16: 107–114.

Hallett PE, Lightstone AD (1976b) Saccadic eye movements towards stimuli triggered by prior saccades. Vision Res. 16: 99–106.

Hanes DP, Schall JD (1996) Neural control of voluntary movement initiation. Science 274: 427–430.

Heide W, Blankenburg M, Zimmermann E, Kompf D (1995) Cortical control of double-step saccades: Implications for spatial orientation. Ann. Neurol. 38: 739–748.

Henriques DY, Klier EM, Smith MA, Lowy D, Crawford JD (1998) Gaze-centered remapping of remembered visual space in an open-loop pointing task. J. Neurosci. 18: 1583–1594.

Herter TM, Guitton D (1998) Human head-free gaze saccades to targets flashed before gaze-pursuit are spatially accurate. J. Neurophysiol. 80: 2785–2789.

Hoddevik GH, Brodal A, Walberg F (1976) The olivocerebellar projection in the cat studied with the method of retrograde axonal transport of horseradish peroxidase. III. The projection to the vermal visual area. J. Comp. Neurol. 169: 155–170.

Ilg UJ, Thier P (2003) Visual tracking neurons in primate area MST are activated by smooth-pursuit eye movements of an "imaginary" target. J. Neurophysiol. 90: 1489–1502.

Jürgens R, Becker W, Kornhuber HH (1981) Natural and drug-induced variations of velocity and duration of human saccadic eye movements: evidence for a control of the neural pulse generator by local feedback. Biol. Cybern. 39: 87–96.

Keller E, Johnsen SD (1990) Velocity prediction in corrective saccades during smooth-pursuit eye movements in monkey. Exp. Brain Res. 80: 525–531.

Keller EL, Crandall WF (1983) Neuronal responses to optokinetic stimuli in pontine nuclei of behaving monkey. J. Neurophysiol. 49: 169–187.

Keller EL, Gandhi NJ, Weir PT (1996) Discharge of superior collicular neurons during saccades made to moving targets. J. Neurophysiol. 76: 3573–3577.

Kim JN, Shadlen MN (1999) Neural correlates of a decision in the dorsolateral prefrontal cortex of the macaque. Nat. Neurosci. 2: 176–185.

Komatsu H, Wurtz RH (1988a) Relation of cortical areas MT and MST to pursuit eye movements. I. Localization and visual properties of neurons. J. Neurophysiol. 60: 580–603.

Komatsu H, Wurtz RH (1988b) Relation of cortical areas MT and MST to pursuit eye movements. III. Interaction with full-field visual stimulation. J. Neurophysiol. 60: 621–644.

Krauzlis RJ (2004) Recasting the smooth pursuit eye movement system. J. Neurophysiol. 91: 591–603.

Krauzlis RJ, Stone LS (1999) Tracking with the mind's eye. Trends Neurosci. 22: 544–550.

Lefèvre P, Quaia C, Optican LM (1998) Distributed model of control of saccades by superior colliculus and cerebellum. Neural Networks 11: 1175–1190.

Leon MI, Shadlen MN (2003) Representation of time by neurons in the posterior parietal cortex of the macaque. Neuron. 38: 317–327.

Lewis JW, Van Essen DC (2000) Corticocortical connections of visual, sensorimotor, and multimodal processing areas in the parietal lobe of the macaque monkey. J. Comp. Neurol. 428: 112–137.

Lewis RF, Zee DS, Hayman MR, Tamargo RJ (2001) Oculomotor function in the rhesus monkey after deafferentation of the extraocular muscles. Exp. Brain Res. 141: 349–358.

Lisberger SG, Fuchs AF (1978a) Role of primate flocculus during rapid behavioral modification of vestibuloocular reflex. I. Purkinje cell activity during visually guided horizontal smooth-pursuit eye movements and passive head rotation. J. Neurophysiol. 41: 733–763.

Lisberger SG, Fuchs AF (1978b) Role of primate flocculus during rapid behavioral modification of vestibuloocular reflex. II. Mossy fiber firing patterns during horizontal head rotation and eye movement. J. Neurophysiol. 41: 764–777.

Maunsell JH, Van Essen DC (1983) Functional properties of neurons in middle temporal visual area of the macaque monkey. I. Selectivity for stimulus direction, speed, and orientation. J. Neurophysiol. 49: 1127–1147.

May JG, Keller EL, Suzuki DA (1988) Smooth-pursuit eye movement deficits with chemical lesions in the dorsolateral pontine nucleus of the monkey. J. Neurophysiol. 59: 952–977.

Mays LE, Sparks DL (1980) Saccades are spatially, not retinocentrically, coded. Science 208: 1163–1165.

Mazurek ME, Roitman JD, Ditterich J, Shadlen MN (2003) A role for neural integrators in perceptual decision making. Cereb. Cortex. 13: 1257–1269.

McKenzie A, Lisberger SG (1986) Properties of signals that determine the amplitude and direction of saccadic eye movements in monkeys. J. Neurophysiol. 56: 196–207.

Medendorp WP, Smith MA, Tweed DB, Crawford JD (2002) Rotational remapping in human spatial memory during eye and head motion. J. Neurosci. 22: RC196.

Merriam EP, Genovese CR, Colby CL (2003) Spatial updating in human parietal cortex. Neuron. 39: 361–373.

Miles FA, Fuller JH (1975) Visual tracking and the primate flocculus. Science 189: 1000–1002.

Missal M, Heinen SJ (2001) Facilitation of smooth pursuit initiation by electrical stimulation in the supplementary eye fields. J. Neurophysiol. 86: 2413–2425.

Missal M, Heinen SJ (2004) Supplementary eye fields stimulation facilitates anticipatory pursuit. J. Neurophysiol. 92: 1257–1262.

Mushiake H, Fujii N, Tanji J (1999) Microstimulation of the lateral wall of the intraparietal sulcus compared with the frontal eye field during oculomotor tasks. J. Neurophysiol. 81: 1443–1448.

Mustari MJ, Fuchs AF, Wallman J (1988) Response properties of dorsolateral pontine units during smooth pursuit in the rhesus macaque. J. Neurophysiol. 60: 664–686.

Nagao S, Kitamura T, Nakamura N, Hiramatsu T, Yamada J (1997) Differences of the primate flocculus and ventral paraflocculus in the mossy and climbing fiber input organization. J. Comp. Neurol. 382: 480–498.

Neal JW, Pearson RCA, Powell TPS (1990) The connections of area PG, 7a, with cortex in the parietal, occipital and temporal lobes of the monkey. Brain Research 532: 249–264.

Newsome WT, Wurtz RH, Dursteler MR, Mikami A (1985) Deficits in visual motion processing following ibotenic acid lesions of the middle temporal visual area of the macaque monkey. J. Neurosci. 5: 825–840.

Newsome WT, Wurtz RH, Komatsu H (1988) Relation of cortical areas MT and MST to pursuit eye movements. II. Differentiation of retinal from extraretinal inputs. J. Neurophysiol. 60: 604–620.

Noda H, Fujikado T (1987) Topography of the oculomotor area of the cerebellar vermis in macaques as determined by microstimulation. J. Neurophysiol. 58: 359–378.

Ohtsuka K (1994) Properties of memory-guided saccades toward targets flashed during smooth pursuit in human subjects. Invest Ophthalmol Vis. Sci. 35: 509–514.

Optican LM, Quaia C (2002) Distributed model of collicular and cerebellar function during saccades. Ann. N Y Acad. Sci. 956: 164–177.

Paré M, Wurtz RH (1997) Monkey posterior parietal cortex neurons antidromically activated from superior colliculus. J. Neurophysiol. 78: 3493–3497.

Pierrot-Deseilligny C, Rivaud S, Gaymard B, Agid Y (1991) Cortical control of memory-guided saccades in man. Exp. Brain Res. 83: 607–617.

Quaia C, Lefèvre P, Optican LM (1999) Model of the control of saccades by superior colliculus and cerebellum. J. Neurophysiol. 82: 999–1018.

Quaia C, Optican LM, Goldberg ME (1998) The maintenance of spatial accuracy by the perisaccadic remapping of visual receptive fields. Neural. Networks 11: 1229–1240.

Rambold H, Churchland A, Selig Y, Jasmin L, Lisberger SG (2002) Partial ablations of the flocculus and ventral paraflocculus in monkeys cause linked deficits in smooth pursuit eye movements and adaptive modification of the VOR. J. Neurophysiol. 87: 912–924.

Rao SM, Mayer AR, Harrington DL (2001) The evolution of brain activation during temporal processing. Nat. Neurosci. 4: 317–323.

Reddi BA, Asrress KN, Carpenter RH (2003) Accuracy, information, and response time in a saccadic decision task. J. Neurophysiol. 90: 3538–3546.

Reddi BA, Carpenter RH (2000) The influence of urgency on decision time. Nat. Neurosci. 3: 827–830.

Robinson DA (1970) Oculomotor unit behavior in the monkey. J. Neurophysiol. 33: 393–403.

Robinson DA (1973) Models of the saccadic eye movement control system. Kybernetik 14: 71–83.

Robinson FR, Fuchs AF (2001) The role of the cerebellum in voluntary eye movements. Annu. Rev. Neurosci. 24: 981–1004.

Roitman JD, Shadlen MN (2002) Response of neurons in the lateral

intraparietal area during a combined visual discrimination reaction time task. J. Neurosci. 22: 9475–9489.
Ruskell GL (1999) Extraocular muscle proprioceptors and proprioception. Prog. Retin. Eye Res. 18: 269–291.
Sakata H, Shibutani H, Kawano K (1983) Functional properties of visual tracking neurons in posterior parietal association cortex of the monkey. J. Neurophysiol. 49: 1364–1380.
Salinas E (2003) Self-sustained activity in networks of gain-modulated neurons. Neurocomputing 52–54: 913–918.
Salinas E, Sejnowski TJ (2001) Gain modulation in the central nervous system: where behavior, neurophysiology, and computation meet. Neuroscientist 7: 430–440.
Salinas E, Thier P (2000) Gain modulation: a major computational principle of the central nervous system. Neuron. 27: 15–21.
Schall JD (2001) Neural basis of deciding, choosing and acting. Nat. Rev. Neurosci. 2: 33–42.
Schall JD, Bichot NP (1998) Neural correlates of visual and motor decision processes. Curr. Opin. Neurobiol. 8: 211–217.
Schall JD, Hanes DP (1998) Neural mechanisms of selection and control of visually guided eye movements. Neural Networks 11: 1241–1251.
Schall JD, Thompson KG (1999) Neural selection and control of visually guided eye movements. Annu. Rev. Neurosci. 22: 241–259.
Schlack A, Hoffmann KP, Bremmer F (2003) Selectivity of macaque ventral intraparietal area (area VIP) for smooth pursuit eye movements. J. Physiol. 551: 551–561.
Schlag J, Schlag-Rey M (1990) Colliding saccades may reveal the secret of their marching orders. Trends Neurosci. 13: 410–415.
Schlag J, Schlag-Rey M, Dassonville P (1989) Interactions between natural and electrically evoked saccades. II. At what time is eye position sampled as a reference for the localization of a target? Exp. Brain Res. 76: 548–558.
Schlag J, Schlag-Rey M, Dassonville P (1990) Saccades can be aimed at the spatial location of targets flashed during pursuit. J. Neurophysiol. 64: 575–581.
Shadlen MN, Newsome WT (1996) Motion perception: seeing and deciding. Proc. Natl. Acad. Sci. USA 93: 628–633.
Smeets JBJ, Bekkering H (2000) Prediction of saccadic amplitude during smooth pursuit eye movements. Human Movement Science 19: 275–295.
Sommer MA (2003) The role of the thalamus in motor control. Curr. Opin. Neurobiol. 13: 663–670.
Sommer MA, Wurtz RH (2002) A pathway in primate brain for internal monitoring of movements. Science 296: 1480–1482.
Sommer MA, Wurtz RH (2004a) What the brain stem tells the frontal cortex. I. Oculomotor signals sent from superior colliculus to frontal eye field via mediodorsal thalamus. J. Neurophysiol. 91: 1381–1402.
Sommer MA, Wurtz RH (2004b) What the brain stem tells the frontal cortex. II. Role of the SC-MD-FEF pathway in corollary discharge. J. Neurophysiol. 91: 1403–1423.
Squatrito S, Maioli MG (1997) Encoding of smooth pursuit direction and eye position by neurons of area MSTd of macaque monkey. J. Neurosci. 17: 3847–3860.
Suzuki DA, Keller EL (1988a) The role of the posterior vermis of monkey cerebellum in smooth-pursuit eye movement control. I. Eye and head movement-related activity. J. Neurophysiol. 59: 1–18.
Suzuki DA, Keller EL (1988b) The role of the posterior vermis of monkey cerebellum in smooth-pursuit eye movement control. II. Target velocity-related Purkinje cell activity. J. Neurophysiol. 59: 19–40.
Suzuki DA, Noda H, Kase M (1981) Visual and pursuit eye movement-related activity in posterior vermis of monkey cerebellum. J. Neurophysiol. 46: 1120–1139.
Suzuki DA, Yamada T, Yee RD (2003) Smooth-pursuit eye-movement-related neuronal activity in macaque nucleus reticularis tegmenti pontis. J. Neurophysiol. 89: 2146–2158.
Takagi M, Zee DS, Tamargo RJ (2000) Effects of lesions of the oculomotor cerebellar vermis on eye movements in primate: smooth pursuit. J. Neurophysiol. 83: 2047–2062.
Tanaka M (2005) Involvement of the central thalamus in the control of smooth pursuit eye movements. J. Neurosci. 25: 5866–5876.
Thier P, Andersen RA (1996) Electrical microstimulation suggests two different forms of representation of head-centered space in the intraparietal sulcus of rhesus monkeys. Proc. Natl. Acad. Sci. USA 93: 4962–4967.
Thier P, Andersen RA (1998) Electrical microstimulation distinguishes distinct saccade-related areas in the posterior parietal cortex. J. Neurophysiol. 80: 1713–1735.
Thier P, Koehler W, Buettner UW (1988) Neuronal activity in the dorsolateral pontine nucleus of the alert monkey modulated by visual stimuli and eye movements. Exp. Brain Res. 70: 496–512.
Thurston SE, Leigh RJ, Crawford T, Thompson A, Kennard C (1988) Two distinct deficits of visual tracking caused by unilateral lesions of cerebral cortex in humans. Ann. Neurol. 23: 266–273.
Tian J, Schlag J, Schlag-Rey M (2000) Testing quasi-visual neurons in the monkey's frontal eye field with the triple-step paradigm. Exp. Brain Res. 130: 433–440.
Tobler PN, Felblinger J, Burki M, Nirkko AC, Ozdoba C, Muri RM (2001) Functional organisation of the saccadic reference system processing extraretinal signals in humans. Vision Res. 41: 1351–1358.
Tusa RJ, Ungerleider LG (1988) Fiber pathways of cortical areas mediating smooth pursuit eye movements in monkeys. Ann. Neurol. 23: 174–183.
Ungerleider LG, Desimone R (1986) Cortical connections of visual area MT in the macaque. J. Comp. Neurol. 248: 190–222.
Van Essen DC, Maunsell JH, Bixby JL (1981) The middle temporal visual area in the macaque: myeloarchitecture, connections, functional properties and topographic organization. J. Comp. Neurol. 199: 293–326.
Van Gisbergen JA, Robinson DA, Gielen S (1981) A quantitative analysis of generation of saccadic eye movements by burst neurons. J. Neurophysiol. 45: 417–442.
Wang XJ (2001) Synaptic reverberation underlying mnemonic persistent activity. Trends Neurosci. 24: 455–463.
Weir CR, Knox PC, Dutton GN (2000) Does extraocular muscle proprioception influence oculomotor control? Br. J. Ophthalmol. 84: 1071–1074.
Wolpert DM, Miall RC, Kawato M (1998) Internal models in the cerebellum. Trends Cogn. Sci. 2: 338–347.
Zhang T, Heuer HW, Britten KH (2004) Parietal area VIP neuronal responses to heading stimuli are encoded in head-centered coordinates. Neuron. 42: 993–1001.
Zivotofsky AZ, Rottach KG, Averbuch-Heller L, Kori AA, Thomas CW, Dell'Osso LF, Leigh RJ (1996) Saccades to remembered targets: the effects of smooth pursuit and illusory stimulus motion. J. Neurophysiol. 76: 3617–3632.